General Disclaimer

One or more of the Following Statements may affect this Document

- This document has been reproduced from the best copy furnished by the organizational source. It is being released in the interest of making available as much information as possible.

- This document may contain data, which exceeds the sheet parameters. It was furnished in this condition by the organizational source and is the best copy available.

- This document may contain tone-on-tone or color graphs, charts and/or pictures, which have been reproduced in black and white.

- This document is paginated as submitted by the original source.

- Portions of this document are not fully legible due to the historical nature of some of the material. However, it is the best reproduction available from the original submission.

A FLUID DESCRIPTION OF PLASMA DOUBLE-LAYERS

by

J. S. Levine and F. W. Crawford

Technical Report

SU-IPR Report No. 787

May 1979

Institute for Plasma Research
Stanford University
Stanford, California 94305

CONTENTS

FIGURE

A.1. Variation of functions F_γ and F_1 (Arrows correspond to $q\phi$ decreasing).

    (a) Adiabatic.

    (b) Isothermal.

B.1. Velocity distribution functions at $q\phi = 0$ and $q\phi < 0$.

    (a) Waterbag with all particles forward-going.

    (b) Waterbag with forward- and backward-going particles.

    (c) Maxwellian with large drift-to-thermal velocity ratio.

    (d) Half-Maxwellian.

B.2. Variation of $N(\phi)$ for the velocity distribution functions of figure B.1.

A FLUID DESCRIPTION OF PLASMA DOUBLE-LAYERS

by

J. S. Levine and F. W. Crawford
Institute for Plasma Research
Stanford University, CA 94305, USA

ABSTRACT

This paper describes the space-charge double-layer that forms
between two plasmas with different densities and thermal energies.
Three progressively more realistic models are treated by fluid theory,
taking into account four species of particles: electrons and ions
reflected by the double-layer, and electrons and ions transmitted
through it. First, the two plasmas are assumed to be cold, and the self-
consistent potential, electric field and space-charge distributions within
the double-layer are determined. Second, the effects of thermal velo-
cities are taken into account for the reflected particles, and the modifi-
cations to the cold plasma solutions are established. Third, the further
modifications due to thermal velocities of the transmitted particles are
examined. The applicability of a one-dimensional fluid description,
rather than plasma kinetic theory, is discussed. One valuable product
of this description is the potential difference across the double-layer
in terms of the parameters of the two plasmas which it separates. A
useful length parameter is defined characterizing the distance over
which most of this potential is dropped. Comparisons are then made
between theoretical predictions, and double-layer potentials and lengths
deduced from laboratory and space plasma experiments.

1

1. INTRODUCTION

Double-layers consist of two space-charge layers in close proximity, one positively charged and one negatively. They are commonly observed in the laboratory as cathode sheaths (Langmuir 1929; Crawford & Cannara 1965; Prewett & Allen 1976), or as constriction sheaths if the vessel containing a plasma column has a reduction in cross-sectional area (Crawford & Freeston 1963; Andersson et al. 1969; Sandahl 1971; Jacobson & Eubank 1973).

Double-layers can occur that are not controlled by electrodes or by the boundary. Laboratory experiments on positive columns in a variety of neutral gases, with (Lutsenko et al. 1975; Torvén & Andersson 1978) and without (Babić & Torvén 1974; Armstrong & Torvén 1974; Armstrong 1975; Levine et al. 1978) magnetic fields, have demonstrated the onset of double-layers as the current density is raised. They have also been observed in double- (Quon & Wong 1976) and triple-plasma (Coakley et al. 1978) devices as transitions between plasmas of differing characteristics, and in various computer simulations of such plasmas (Goertz & Joyce 1975; DeGroot et al. 1977; Joyce & Hubbard 1978; Hubbard & Joyce 1978). The experimental evidence for double-layers has been reviewed by Torvén (1978). There is a growing body of evidence that double-layers form in the magnetosphere, accelerating the high energy electrons that are associated with auroral displays (see, e.g. Shawhan et al. 1978 and references therein). Double-layers have also been invoked in discussions of solar flares (Alfvén & Carlqvist 1967; Carlqvist 1969; Hasan & ter Haar 1978), and to explain how Io modulates Jovian decametric radiation (Smith & Goertz 1978).

A variety of theoretical models of state-state double-layers have been proposed which can be understood qualitatively from figure 1(a): a monotonic potential variation occurs over a length that is long on the scale of the electron and ion Debye lengths, but small on the scale of laboratory or space dimensions. The localization of the potential step, and the associated electric field, implies that although neutrality is violated within the double-layer, the charge, integrated across the double-layer, is zero. The plasmas in Regions 1 and 2 may be characterized by different densities, drift velocities and temperatures. The double-layer is assumed to be much shorter than the collisional mean free path, so that

collision effects within it may be ignored, though they may be important
in Regions 1 and 2. The double-layer is generally treated as a one-
dimensional structure, thus excluding magnetic field effects, but a two-
dimensional model in which the double-layer is oblique to the magnetic
field, has been treated (Swift 1975). A general review of double-layer
theory has been given by Carlqvist (1978).

Several specific models of double-layers that have been studied are
shown in figure 1(b)-(e). In the first of these, Region 1 is replaced by
an electron-emitting cathode, injecting a flux Γ_e of cold electrons, and
Region 2 is replaced by an ion-emitting anode, injecting a flux Γ_i of
cold ions, as shown in figure 1(b). The Langmuir (1929) theory of a space-
charge-limited diode can be applied to the double-layer. In this, Poisson's
equation is solved consistently with the particle fluxe". The well known
Langmuir relation, $\Gamma_e/\Gamma_i = (m_i/m_e)^{1/2}$, is derived from the assumption that
the electric field vanishes at the emitting surfaces.

In a model studied by Crawford & Cannara (1965), appropriate to a hot
cathode discharge, Region 1 is replaced by an electron-emitting cathode,
and Region 2 is taken to be a uniform infinite plasma, as illustrated in
figure 1(c). Plasma electrons reflected within the sheath are assumed to
obey Boltzmann's law. Ions entering the double-layer from the plasma are
taken as monoenergetic. A minimum ion velocity is found which, in the
limit of a low flux of electrons injected from the cathode, is the Bohm
(1949) sheath condition, $v_i^2 > T_e/m_i$.

Block (1972) treats the double-layer between two infinite plasmas,
using fluid theory to include temperature effects, and taking account of
a population of ions in Region 1, and of electrons in Region 2, that are
reflected by the potential step, as shown in figure 1(d). For the case of
an infinite potential difference across the double-layer, Block shows that
the Langmuir condition is obeyed, and that modified Bohm conditions must
be satisfied for the model to be self-consistent.

Montgomery & Joyce (1969) use kinetic theory to show that a double-
layer may be constructed as a stationary shock-like solution of the Vlasov
equation in a system with no current. As illustrated in figure 1(e), they
assume two streaming populations in Region 1; electrons that are accelerated
by the potential, and ions of the same density and velocity that are decele-
rated, but transmitted through the double-layer. A second electron

population is required on the high potential side of the double-layer to ensure electrical neutrality. The transmission of the ions imposes an upper limit on the potential difference equal to the ion streaming energy.

Kan (1975) extends the Montgomery & Joyce (1969) model to show that electrostatic shock solutions can exist in a $T_i \gg T_e$ plasma under conditions of the high latitude plasma sheet. Populations of reflected ions in Region 1 and transmitted ions from Region 2 are included, and the assumption of zero current is eliminated. Magnetic field effects are treated in this one-dimensional theory by using loss-cone distribution functions. Necessary conditions for existence of the shock are derived in terms of the ratios of drift to thermal velocity for ions and electrons, for an assumed potential difference.

Andrews & Allen (1971) describe double-layers in terms of averages over unspecified distribution functions, and use Maxwellian distributions for the reflected particles, as in figure 1(d). Numerical results for transmitted particles with delta-function distributions are presented, which satisfy Bohm conditions, but give values of Γ_e/Γ_i that are less than the Langmuir condition.

Hasan & ter Haar (1978) analyze the double-layer for delta-function and power law distributions for the transmitted particles in figure 1(d), using waterbag distributions for the reflected particles. Conditions analogous to the Bohm conditions are derived, and a modified Langmuir condition is derived for delta-function distributions of transmitted particles.

Using a different approach, Knorr & Goertz (1974) assume forms for the potential and for the velocity distributions of three of the four particle species in figure 1(d), and then show that the fourth velocity distribution can be found self-consistently. By setting the reflected ion population to zero, and applying the Penrose (1960) criterion, they show that the plasma is stable against small perturbations if the double-layer is long enough, and the transmitted ion population is fast enough.

In this paper, the double-layer is analyzed using fluid theory. Section 2 treats the case of cold particles; thermal effects for the reflected particles are included in §3, and for the transmitted particles in §4. The emphasis is on finding a relationship between the magnitude of the potential step, and the parameters characterizing the adjoining plasmas. In §5, qualitative statements are made about the length of the double-layer and a characteristic length useful as a quantitative measure is defined and discussed.

2. COLD PLASMAS

As a starting point, all of the particles in figure 1(d) are taken to be at zero temperature. The "reflected" particles are actually stationary, and cannot penetrate the double-layer. Consequently, only transmitted particles need be considered in establishing the self-consistent potential. The density of the stationary particles will be determined so as to satisfy neutrality outside the double-layer.

Electrons enter the double-layer from Region 1 with velocity u_{e1}, density n_{e1} and flux $\Gamma_e(= n_{e1}u_{e1})$. Ions from Region 2 enter with velocity u_{i2}, density n_{i2} and flux $\Gamma_i(= n_{i2}u_{i2})$. At a point, x, within the double-layer, where the potential is ϕ, the particle velocities and densities, determined from conservation of energy and particle flux, are

$$u_e(x) = \left(u_{e1}^2 + \frac{2e\phi}{m_e}\right)^{1/2} \quad , \quad u_i(x) = \left(u_{i2}^2 + \frac{2e}{m_i}(\phi_0-\phi)\right)^{1/2} \quad ,$$

$$n_e(x) = \frac{\Gamma_e}{\left(u_{e1}^2 + \frac{2e\phi}{m_e}\right)^{1/2}} \quad , \quad n_i(x) = \frac{\Gamma_i}{\left(u_{i2}^2 + \frac{2e}{m_i}(\phi_0-\phi)\right)^{1/2}} \quad , \quad (1)$$

where $m_e(m_i)$ is the electron (ion) mass, and e is the magnitude of the electronic charge. Substituting the densities from Eq. (1) in Poisson's equation yields,

$$\frac{d^2\phi}{dx^2} = \frac{e}{\epsilon_0}(n_e-n_i) = \frac{e}{\epsilon_0}\left(\frac{\Gamma_e}{\left(u_{ei}^2 + \frac{2e\phi}{m_e}\right)^{1/2}} - \frac{\Gamma_i}{\left(u_{i2}^2 + \frac{2e(\phi_0-\phi)}{m_i}\right)^{1/2}}\right). \quad (2)$$

Equation (2) can be used to define a function $P(\phi)$ such that

$$\frac{d^2\phi}{dx^2} \equiv -\frac{dP}{d\phi}. \quad (3)$$

Integrating, we obtain

$$P(\phi) = -\frac{1}{\epsilon_0}\left\{ m_e \Gamma_e \left[\left(u_{e1}^2 + \frac{2e\phi}{m_e}\right)^{1/2} - u_{e1}\right]\right.$$

$$\left. + m_i \Gamma_i \left[\left(u_{12}^2 + \frac{2e}{m_i}(\phi_0-\phi)\right)^{1/2} - \left(u_{12}^2 + \frac{2e}{m_i}\phi_0\right)^{1/2}\right]\right\}, \tag{4}$$

where the constant of integration is chosen so that $P(0) = 0$. Alternatively, P can be expressed as

$$P(x) = \frac{E^2(0) - E^2(x)}{2} = -\int_0^x \rho(x')E(x')dx'. \tag{5}$$

The electric field is assumed to vanish at the edges of the double-layer,

$$E(0) = E(x_1) = 0. \tag{6}$$

This ensures that the charge density integrated across the double-layer vanishes. The function P is thus constrained to satisfy

$$P(x_1) = 0, \qquad P(\phi_0) = 0, \tag{7}$$

and is negative within the double-layer. Since the integrand in the last equality in Eq. (5) is the force between the double-layer and the particles, Eq. (7) can be viewed as a statement of mechanical equilibrium.

Setting $P(\phi_0) = 0$ in Eq. (4) yields

$$\phi_0 = 2M\Gamma_e\Gamma_i \frac{(\Gamma_e u_{e1} - M\Gamma_i u_{12})(\Gamma_i u_{e1} - \Gamma_e u_{12})}{(\Gamma_e^2 - M\Gamma_i^2)^2}, \tag{8}$$

where $M = m_i/m_e$. Although Eq. (8) predicts a positive value for ϕ_0 within the ranges

$$\frac{u_{e1}^2}{u_{12}^2} > \frac{\Gamma_e u_{e1}}{\Gamma_i u_{12}} > M, \qquad \frac{u_{e1}^2}{u_{12}^2} < \frac{\Gamma_e u_{e1}}{\Gamma_i u_{12}} < M, \tag{9}$$

the actual range is more restrictive. This can be seen by solving $P(\phi_0) = 0$ for Γ_e/Γ_i,

$$\frac{\Gamma_e}{\Gamma_i} = M \left(\frac{u_{12}}{u_{el}}\right) \left[\frac{\left(1 + \frac{2e\phi_0}{m_i u_{12}^2}\right)^{1/2} - 1}{\left(1 + \frac{2e\phi_0}{m_e u_{el}^2}\right)^{1/2} - 1}\right], \tag{10}$$

which varies monotonically from u_{el}/u_{12} to $M^{1/2}$ as ϕ_0 varies from zero to infinity. The ranges of possible double-layer solutions are thus

$$\frac{u_{el}^2}{u_{12}^2} > \frac{\Gamma_e^2}{\Gamma_i^2} > M \quad, \quad \frac{u_{el}^2}{u_{12}^2} < \frac{\Gamma_e^2}{\Gamma_i^2} < M \ . \tag{11}$$

Langmuir's model (Langmuir 1929; Block 1972) of the space-charge-limited diode is contained in this formalism as a special case. Finite fluxes of particles enter the double-layer with zero velocity, so that the numerator of Eq. (8) vanishes. (The emissive powers of the cathode and the anode are assumed infinite.) Therefore $\phi_0 \neq 0$ can be obtained only if the denominator also vanishes. This yields the Langmuir (1929) condition

$$\Gamma_e/\Gamma_i = (m_i/m_e)^{1/2} \ , \tag{12}$$

and leaves the potential difference indeterminate.

Equation (8) may be rewritten with the fluxes eliminated in favor of the particle densities,

$$\Phi_0 = 2NQ \frac{(1-NQ)(N-1)}{(1-N^2Q)^2} \ , \tag{13}$$

where we have introduced the normalization

$$\Phi = \frac{e\phi}{m_e u_{el}^2}, \quad N = \frac{n_{12}}{n_{el}}, \quad Q = \frac{m_i u_{12}^2}{m_e u_{el}^2} \ . \tag{14}$$

Equation (11) reduces to the limits

$$N > 1 > N^2 Q \quad , \quad N < 1 < N^2 Q \, . \tag{15}$$

These regions in (N,Q) space are shown shaded in figure 2.

For neutrality in Plasmas 1 and 2, the reflected particle populations, normalized to n_{e1}, must satisfy

$$\eta_i = \frac{n_{i1}}{n_{e1}} = 1 - \frac{N}{\left(1 + \frac{2}{Q}\phi_0\right)^{1/2}} \quad , \quad \eta_e = \frac{n_{e2}}{n_{e1}} = N - \frac{1}{\left(1 + 2\phi_0\right)^{1/2}} \quad , \tag{16}$$

where n_{i1} is the density of reflected ions in Plasma 1 and n_{e2} is the density of reflected electrons in Plasma 2. Since η_i and η_e represent particle densities, they must not be negative. For $N < 1$, η_i is always positive, while for $N > 1$, η_e is always positive. Using Eq. (13), and examining the non-trivial cases yields

$$N^2 Q > \frac{N+1}{3-N} \quad (N < 1) ; \qquad N^2 Q < \frac{3N-1}{N+1} \qquad (N > 1) \, . \tag{17}$$

The conditions of Eq. (17) are less stringent than those for existence of a double-layer, Eq. (15). It follows that for double-layer formation there must be reflected particles on both sides of the double-layer.

Figure 3(a) shows the electrical potential, $\phi(Z)$, electric field, $E(Z)$, and charge density, $\rho(Z)$, for $N = 1.1$ and $Q = 0.8$. The normalization for the spatial coordinate, Z, is

$$Z = x \left(\frac{n_{e1} e^2}{m \, \epsilon_0 \, u_{e1}^2} \right)^{1/2} \, . \tag{18}$$

The electric field and charge density are normalized so that $\rho = dE/dZ = -d^2\phi/dZ^2$.

Although the precise spatial variation of the electric potential can be determined only by integration of Eq. (3), some symmetry properties can be deduced from the function Π ,

$$\Pi = \frac{\epsilon_0 P}{m_e n_{el} u_{el}^2} = 1 - (1 + 2\phi)^{1/2} - NQ\left[\left(1 + \frac{2}{Q}(\phi_0 - \phi)\right)^{1/2} - \left(1 + \frac{2}{Q}\phi_0\right)^{1/2}\right]. \tag{19}$$

For the electric potential to be symmetric about $\phi_0/2$, Π must also be symmetric about $\phi_0/2$. This is equivalent to requiring all odd derivatives to vanish at that point,

$$\frac{d^m \Pi}{d\phi^m}\Bigg|_{\phi_0/2} = (2m-3)!!\left[\frac{N}{Q^{m-1}}\left(1 + \frac{\phi_0}{Q}\right)^{\frac{1-2m}{m}} + [-1]^m (1 + \phi_0)^{\frac{1-2m}{m}}\right] = 0, \tag{20}$$

$$(m \text{ odd}).$$

This rearranges to

$$\frac{1 + \phi_0}{1 + \frac{\phi_0}{Q}} = \left(\frac{N}{Q^{m-1}}\right)^{\frac{2}{1-2m}}, \tag{21}$$

which is satisfied by $N = Q = 1$ or $N^2 Q = 1$, where $\phi_0 \to \infty$, only. The asymmetry of the electric potential can be gauged by determining the value of ϕ_M at which the minimum of Π occurs; this corresponds to vanishing charge density and thus to the maximum electric field,

$$\frac{\phi_M}{\phi_0} = \frac{N^3 Q + N^2 Q - 3N + 1}{4N(NQ-1)}. \tag{22}$$

By expanding for weak ($N \approx 1$) and strong ($N^2 Q \approx 1$) double-layers, these cases are found to be nearly symmetrical,

$$\frac{\phi_M}{\phi_0} \approx \frac{1}{2} + \frac{\delta}{4} \quad (N = 1 + \delta), \qquad \frac{\phi_M}{\phi_0} \approx \frac{1}{2} - \frac{\delta}{4} \quad (N^2 Q = 1 + \delta). \tag{23}$$

Contour plots of ϕ_M/ϕ_0 in the (N, Q) plane are shown in figure 4, and indicate $\phi_M/\phi_0 \approx 1/2$ over a broad range of N and Q.

To summarize the foregoing results for cold particles, we note that the double-layer may be completely characterized by the densities and energies of the ions and electrons streaming into it. The densities of the stationary, "reflected" particles, and the magnitude and spatial variation of the electric potential, are uniquely determined.

9

3. REFLECTED PARTICLE TEMPERATURE NON-ZERO

Thermal spread of the reflected particles will be described by assuming a Boltzmann distribution within the double-layer. The temperatures of the reflected ions and electrons, expressed in energy units, are T_{i1} and T_{e2}, respectively. Although this allows an exponentially small number of "reflected" particles to cross the double-layer, for T_{i1}, $T_{e2} \ll e\phi_0$, this error will be negligible.

The non-zero temperature of the reflected particles allows them to penetrate and partially neutralize the double-layer. The sharp boundaries associated with cold particles are thus smoothed out. The potential drop across the double-layer is also affected.

The normalized Poisson equation is

$$\frac{d^2\phi}{dZ^2} = -\frac{d\Pi}{d\phi} = \left\{ \frac{1}{(1+2\phi)^{1/2}} + \eta_e \exp\left(-\frac{\phi_0-\phi}{\mathfrak{I}_e}\right)\right\} - \left\{ \frac{N}{\left(1 + \frac{2}{Q}(\phi_0-\phi)\right)^{1/2}} + \eta_i \exp\left(-\frac{\phi}{\mathfrak{I}_i}\right)\right\},$$

(24)

where $\mathfrak{I}_i \left(= T_{i1}/m_e u_{el}^2\right)$ and $\mathfrak{I}_e \left(= T_{e2}/m_e u_{el}^2\right)$ are the normalized ion and electron temperatures.

Equation (24) is integrated to find Π, corrected for the non-zero reflected particle temperatures. Noting that Eq. (16) is still the proper identification for η_e and η_i, it is found that

$$\Pi(\phi) = 1 - (1+2\phi)^{1/2} + \mathfrak{I}_e\left(N - \frac{1}{(1+2\phi_0)^{1/2}}\right)\left(\exp\left(-\frac{\phi_0}{\mathfrak{I}_e}\right) - \exp\left(-\frac{\phi_0-\phi}{\mathfrak{I}_e}\right)\right)$$

$$- NQ\left[\left(1 + \frac{2}{Q}(\phi_0-\phi)\right)^{1/2} - \left(1 + \frac{2}{Q}\phi_0\right)^{1/2}\right]$$

$$- \mathfrak{I}_i\left(1 - \frac{N}{\left(1 + \frac{2}{Q}\phi_0\right)^{1/2}}\right)\left(\exp\left(-\frac{\phi}{\mathfrak{I}_i}\right) - 1\right).$$

(25)

The self-consistent value, Φ_0, is again determined from the requirement $\Pi(\Phi_0) = 0$. In this case, Φ_0 must be found numerically. For very low temperatures, an approximation to the difference, $\delta\Phi$, between the true value, Φ_0, and that based on Eq. (13), Φ_c, for cold particles, is found to be

$$\delta\Phi = -\mathcal{J}_e \left[\frac{N(1+2\Phi_c)^{1/2} - 1}{N(1+2\Phi_c)^{1/2}\left(1 + \frac{2}{Q}\Phi_c\right)^{-1/2} - 1} \right] + \mathcal{J}_i \left[\frac{\left(1 + \frac{2}{Q}\Phi_c\right)^{1/2} - N}{\left(1 + \frac{2}{Q}\Phi_c\right)^{1/2}(1+2\Phi_c)^{-1/2} - N} \right].$$

(26)

At either edge of the double-layer, both Π and $d\Pi/d\Phi$ vanish; near the edge, Π is thus approximately

$$\Pi(\Phi) \approx \frac{(\Phi-\hat{\Phi})^2}{2} \left. \frac{d^2\Pi}{d\Phi^2}\right|_{\Phi=\hat{\Phi}} \qquad (\hat{\Phi}=0, \Phi_0) .$$

(27)

Since Π must be negative within the double-layer, $d^2\Pi/d\Phi^2$ is required to be negative at $\Phi=0, \Phi_0$. From Eq. (25) the derivative is

$$\frac{d^2\Pi}{d\Phi^2} = (1 + 2\Phi)^{-3/2} - \frac{\eta_e}{\mathcal{J}_e} \exp\left(- \frac{(\Phi_0-\Phi)}{\mathcal{J}_e}\right) + \frac{N}{Q}\left(1 + \frac{2}{Q}(\Phi_0-\Phi)\right)^{-3/2} - \frac{\eta_i}{\mathcal{J}_i} \exp\left(- \frac{\Phi}{\mathcal{J}_i}\right).$$

(28)

This reduces to

$$\mathcal{J}_i < \frac{1 - N\left(1 + \frac{2}{Q}\Phi_0\right)^{-1/2}}{1 + \frac{N}{Q}\left(1 + \frac{2}{Q}\Phi_0\right)^{-3/2}} \quad (\Phi=0), \qquad \mathcal{J}_e < \frac{N - (1 + 2\Phi_0)^{-1/2}}{\frac{N}{Q} + (1 + 2\Phi_0)^{-3/2}} \quad (\Phi=\Phi_0) .$$

(29)

The temperatures are thus bounded from above, $\mathcal{J}_i < 1$ and $\mathcal{J}_e < Q$. In terms of unnormalized variables, these become $T_{i1} < m_e u_{e1}^2$ and $T_{e2} < m_i u_{i2}^2$, which may be recognized as Bohm (1949) conditions for collection of electrons and ions, respectively, through a sheath.

The limits expressed by Eq. (29) must be compared with the physical requirement that the trapped particle densities not be negative. Considering N as the dependent variable, and Φ_0 as an independent variable, Eq. (29) may be rewritten as

11

$$\frac{(1-\mathfrak{I}_i)\left(1 + \frac{2}{Q}\,\Phi_0\right)^{1/2}}{1 + \frac{\mathfrak{I}_i}{Q+2\Phi_0}} > N > \frac{Q\left(1 + \frac{\mathfrak{I}_e}{1 + 2\Phi_0}\right)}{(Q-\mathfrak{I}_e)(1 + 2\Phi_0)^{1/2}} \ . \tag{30}$$

These bounds on N are more stringent than those derived from the require-
ment that the trapped particle densities not be negative,

$$\left(1 + \frac{2}{Q}\,\Phi_0\right)^{1/2} > N > \frac{1}{(1 + 2\Phi_0)^{1/2}} \ . \tag{31}$$

As for cold particles, a self-consistent solution for the double-layer
requires trapped particles on both sides of the double-layer.

Figure 3(b) shows $\Phi(Z)$, $E(Z)$ and $\rho(Z)$ for the values of N and Q
used in figure 3(a), but with warm reflected particles. The penetration
of the double-layer by the reflected particles produces the smooth variations
of Φ , E and ρ .

Examination of $\Pi(\Phi_0)$ for small Φ_0 indicates the possible existence
of a new root $\Pi(\Phi_0) = 0$, and thus a new double-layer solution (see figure 5).
If the solution satisfies Eq. (30), it is physically admissible. The cause
of this modification may be identified by considering $\Pi(\Phi_0)$ as a function
of Φ_0 , and evaluating its derivative at $\Phi_0 = 0$ from Eq. (25). We obtain

$$\left.\frac{d\Pi(\Phi_0)}{d\Phi_0}\right|_{\Phi_0=0} = 1 - N \ . \tag{32}$$

This compares with $d\Pi(\Phi_0)/d\Phi_0 = N-1$ at $\Phi_0 = 0$ when the reflected
particles are cold, as can be seen from Eq. (19). Each of the reflected
species contributes a term $1-N$, so that the slope of $\Pi(\Phi_0)$ is changed
in sign by the inclusion of non-zero temperatures.

If only one of the thermal terms is retained, the first derivative
vanishes and the second derivative is found to be

$$\left.\frac{d^2\Pi(\Phi_0)}{d\Phi_0^2}\right|_{\Phi_0=0} = \begin{cases} \dfrac{N-1}{\mathfrak{I}_e} - \dfrac{N}{Q} - 1 & (\mathfrak{I}_e \neq 0) \ , \\[4mm] \dfrac{N-1}{\mathfrak{I}_i} + \dfrac{N}{Q} + 1 & (\mathfrak{I}_i \neq 0) \ . \end{cases} \tag{33}$$

The value of $\Pi(\Phi_0)$ as Φ_0 approaches infinity is unaffected by the finite temperatures:

$$\Pi(\Phi_0) \to (2\Phi_0)^{1/2} (NQ^{1/2} - 1) \qquad (\Phi_0 \to \infty) . \tag{34}$$

For example, if the initial slope of $\Pi(\Phi_0)$ is negative [$N > 1$, from Eq. (32)] and the asymptotic value is positive [$N^2Q > 1$, from Eq. (34)], there must be at least one root (in general, an odd number of roots) $\Pi(\Phi_0) = 0$. The analysis based on cold particles excluded any roots in this case. Similar reasoning shows that in the ranges limited by the cold particle analysis, $N \gtrless 1 \gtrless N^2Q$, there will be either two roots or none (in general, an even number of roots).

Figure 6 shows the behavior of Φ_0 as J_e and J_i are separately increased from zero. The curves marked $\overline{J}_e$ and $\overline{J}_i$ are based on the linear approximation, Eq. (26). It is seen that Φ_0 decreases with increasing J_e for $N > 1$ and with increasing J_i for $N < 1$. The upper bound on the temperature for these cases comes from Eq. (29), and not from the Bohm conditions, which are its high-potential limits. For certain values of N and Q, the second double-layer solution introduced by the non-zero temperature is physically admissible. As figure 7 shows, the two roots $\Pi(\Phi_0) = 0$ coalesce at a finite Φ_0 and then disappear.

Figure 8 shows (shaded) the regions in (N,Q) space within which double-layer solutions can be found for non-zero reflected particle temperatures. The boundary at $N = 1(\Phi_0 = 0)$ for cold particles is found to vary with temperature. The value of Φ_0 along this boundary also varies, but is everywhere greater than zero. The $N^2Q = 1$ boundary, with infinite Φ_0, is unaffected by the inclusion of temperature.

To establish the validity of the double-layer solutions along the low potential boundary, an additional criterion should be investigated. If Φ_0 is not significantly greater than the reflected particle temperatures, a considerable fraction of the "reflected" particles will be transmitted through the double-layer, thus invalidating the model. In fact, all points along the boundary are found to satisfy $\Phi_0 > J$. For reference, the line $\Phi_0 = 5J$ is shown in figure 8.

4. TRANSMITTED PARTICLE TEMPERATURE NON-ZERO

If the transmitted particle velocity distributions have narrow widths about their streaming velocities, a fluid model can be used to describe the particle dynamics. Denoting the electron temperature by T_e, with value T_{e1} within Plasma 1, and the ion temperature by T_i, with value T_{i2} within Plasma 2, the momentum transfer equations are

$$m_e \frac{d}{dx}\left(\frac{u_e^2}{2}\right) = e\frac{d\phi}{dx} - \frac{1}{n_e}\frac{dp_e}{dx} , \qquad p_e = n_e T_e ,$$

$$m_i \frac{d}{dx}\left(\frac{u_i^2}{2}\right) = -e\frac{d\phi}{dx} - \frac{1}{n_i}\frac{dp_i}{dx} , \qquad p_i = n_i T_i . \tag{35}$$

Assuming that the particles are accelerated adiabatically,

$$\frac{dT}{T} = (\gamma-1)\frac{dn}{n} = 2\frac{dn}{n} , \tag{36}$$

where $\gamma=3$ for one-dimensional adiabatic acceleration, the thermal terms on the right-hand side of Eq. (35) are

$$\frac{1}{n}\frac{d}{dx}(nT) = \frac{3}{2}\frac{dT}{dx} = \frac{3}{2}\frac{d}{dx}\left(\hat{T}\left(\frac{n}{\hat{n}}\right)^2\right) , \tag{37}$$

where $\hat{T}$ and $\hat{n}$ are evaluated at some reference position. Using the continuity of particle flux for each species,

$$u = \frac{\hat{u}\hat{n}}{n} , \tag{38}$$

and Eq. (37), Eq. (35) can be written as a conservation principle,

$$\frac{d}{dx}\left(\frac{n_{e1}^2 u_{e1}^2}{2n_e^2} - \frac{e}{m_e}\phi + \frac{3T_{e1}}{2m_e}\frac{n_e^2}{n_{e1}^2}\right) = 0 ,$$

$$\frac{d}{dx}\left(\frac{n_{i2}^2 u_{i2}^2}{2n_i^2} + \frac{e}{m_i}\phi + \frac{3T_{i2}}{2m_i}\frac{n_i^2}{n_{i2}^2}\right) = 0 . \tag{39}$$

With the normalization given in §2, the conserved quantities become

$$\frac{1}{2N_e^2} - \Phi + \frac{3}{2}\tau_e N_e^2 = \text{const}, \qquad \frac{N^2 Q}{2N_i^2} + \Phi + \frac{3}{2}\tau_i \frac{N_i^2}{N^2} = \text{const}, \tag{40}$$

where the normalized temperatures and densities are

$$\tau_e = \frac{T_{e1}}{m_e u_{e1}^2}, \quad \tau_i = \frac{T_{i2}}{m_e u_{e1}^2}, \quad N_e = \frac{n_e}{n_{e1}}, \quad N_i = \frac{n_i}{n_{e1}}. \tag{41}$$

The constants in Eq. (40) are found by evaluating the left-hand sides in Plasmas 1 and 2 for the electrons and ions, respectively. The expressions in (40) can be solved to yield

$$N_e^2(\Phi) = \frac{2\Phi + 3\tau_e + 1 - \left[(2\Phi + 3\tau_e + 1)^2 - 12\,\tau_e\right]^{1/2}}{6\,\tau_e}, \tag{42}$$

$$N_i^2(\Phi) = N^2 \left[\frac{2(\Phi_0 - \Phi) + 3\tau_i + Q - \left[(2(\Phi_0 - \Phi) + 3\tau_i + Q)^2 - 12\,\tau_i Q\right]^{1/2}}{6\,\tau_i} \right].$$

These expressions are valid only for

$$3\,\tau_e < 1, \quad 3\,\tau_i < Q. \tag{43}$$

For higher temperatures, the fluid approach breaks down, as discussed in Appendix A.

The densities given by Eq. (42) can be used in Poisson's equation to generate a new function Π. The requirement of neutrality outside the double-layer, i.e. that $d\Pi/d\Phi$ vanish at $\Phi = 0$, Φ_0, yields appropriate values for the reflected particle densities,

$$\eta_i = 1 - N \left[\frac{2\Phi_0 + 3\tau_i + Q - \left[(2\Phi_0 + 3\tau_i + Q)^2 - 12\tau_i Q\right]^{1/2}}{6\,\tau_i} \right]^{1/2},$$

$$\eta_e = N - \left[\frac{2\Phi_0 + 3\tau_e + 1 - \left[(2\Phi_0 + 3\tau_e + 1)^2 - 12\tau_e\right]^{1/2}}{6\,\tau_e} \right]^{1/2}. \tag{44}$$

15

The function Π can be divided into four components, one for each of the transmitted and reflected classes of electrons and ions,

$$\Pi = \Pi_{e1} + \Pi_{e2} + \Pi_{i1} + \Pi_{i2} ,$$

$$\Pi_{e1} = 1 - \frac{1}{N_e(\Phi)} + \tau_e \left(1 - N_e^3(\Phi)\right) ,$$

$$\Pi_{e2} = \eta_e \mathcal{J}_e \left[\exp\left(-\frac{\Phi_0}{\mathcal{J}_e}\right) - \exp\left(-\frac{\Phi_0 - \Phi}{\mathcal{J}_e}\right) \right] ,$$

$$\Pi_{i1} = \eta_i \mathcal{J}_i \left(1 - \exp\left(-\frac{\Phi}{\mathcal{J}_i}\right)\right) ,$$

$$\Pi_{i2} = N^2 Q \left(\frac{1}{N_i(0)} - \frac{1}{N_i(\Phi)}\right) + \frac{\tau_i}{N^2} \left(N_i^3(0) - N_i^3(\Phi)\right) . \tag{45}$$

The self-consistent value of the potential step, Φ_0, must again be found numerically. Noting that $d\Pi(\Phi_0)/d\Phi_0 = 1 - N$ at $\Phi_0 = 0$, and that $\Pi \rightarrow (2\Phi_0)^{1/2}(NQ^{1/2} - 1)$ as $\Phi_0 \rightarrow \infty$, we see that the gross behavior of $\Pi(\Phi_0)$ is unaffected by the inclusion of the transmitted particle temperatures. No new double-layer solutions are to be expected, though their location and physical admissibility may be modified.

The change, $\delta\Phi$, between the value predicted for cold particles, Φ_c, and the true Φ_0 can be approximated for small τ_e and τ_i by

$$\delta\Phi \simeq \tau_e \left[\frac{1 - \frac{3}{2}(1+2\Phi_c)^{-1/2} + \frac{1}{2}(1+2\Phi_c)^{-3/2}}{(1+2\Phi_c)^{-1/2} - N\left(1 + \frac{2}{Q}\Phi_c\right)^{-1/2}} \right]$$

$$+ \tau_i N \left[\frac{1 - \frac{3}{2}\left(1 + \frac{2}{Q}\Phi_c\right)^{-1/2} + \frac{1}{2}\left(1 + \frac{2}{Q}\Phi_c\right)^{-3/2}}{N\left(1 + \frac{2}{Q}\Phi_c\right)^{-1/2} - (1 + 2\Phi_c)^{-1/2}} \right] . \tag{46}$$

Equations (26) and (46) are additive when all four species have finite temperatures.

Figure 6 shows the variation of Φ_0 as τ_e and τ_i are separately increased from zero. The curves marked $\overline{\tau}_e$ and $\overline{\tau}_i$ are based on the

linear approximation, Eq. (46). The qualitative effects are similar to those for non-zero J_e and J_i, though Φ_0 is not double-valued and has no low potential cutoff. The condition $d^2\Pi/d\Phi^2 < 0$ for $\Phi = 0$, Φ_0 becomes

$$-\frac{dN_e}{d\Phi} - \frac{\eta_e}{J_e} \exp\left(-\frac{\Phi_0-\Phi}{J_e}\right) - \frac{\eta_i}{J_i} \exp\left(-\frac{\Phi}{J_i}\right) + \frac{dN_i}{d\Phi} < 0 \quad (\Phi = 0, \Phi_0) , \quad (47)$$

where $dN_e/d\Phi$ and $dN_i/d\Phi$ are evaluated from Eq. (42),

$$\frac{dN_e}{d\Phi} = -\left[\frac{2\Phi + 3\tau_e + 1 - \left[(2\Phi + 3\tau_e + 1)^2 - 12\tau_e\right]^{1/2}}{6\tau_e\left[(2\Phi + 3\tau_e + 1)^2 - 12\tau_e\right]}\right]^{1/2} , \quad (48)$$

$$\frac{dN_i}{d\Phi} = N\left[\frac{2(\Phi_0-\Phi) + 3\tau_i + Q - \left(2(\Phi_0-\Phi) + 3\tau_i +Q\right)^2 - 12\tau_iQ\right]^{1/2}}{6\tau_i\left[\left(2(\Phi_0-\Phi) + 3\tau_i + Q\right)^2 - 12\tau_iQ\right]}\right]^{1/2} .$$

Since $dN_e/d\Phi$ is negative and $dN_i/d\Phi$ is positive, i.e. electrons become less dense and ions more dense in moving to higher potential, η_e and η_i have positive lower bounds. In the limit of strong double-layers, $\Phi_0 \to \infty$, Eq. (47) reduces to

$$J_i + 3\tau_e < 1 \quad (\Phi=0) , \quad J_e + 3\tau_i < Q \quad (\Phi=\Phi_0) , \quad (49)$$

or, in terms of unnormalized variables

$$T_{i1} + 3T_{e1} < m_e u_{e1}^2 , \quad T_{e2} + 3T_{i2} < m_i u_{i2}^2 . \quad (50)$$

These upper bounds apply only in the infinite potential limit; for finite potentials, Eq. (47) is more restrictive and is thus the appropriate criterion to be applied.

If the reflected particles are cold, $d\Pi/d\Phi$ is discontinuous at $\Phi = 0$, Φ_0 even though the transmitted particles are warm. Equation (47) is then replaced by the requirement that the density of the reflected particles, [η_i, η_e from Eq. (44)], not be negative.

5. DOUBLE-LAYER DIMENSIONS

Having determined how the potential drop, Φ_0 , of the double-layer depends on the physical parameters of the adjoining plasmas, the remaining question accessible to this analysis is how the spatial extent of the double-layer is determined.

In determining the distance required for the potential to vary from 0 to Φ_0 , two distinct cases can be distinguished by making a power-series expansion for Π . If the reflected particles are cold, the charge density, $\rho(= d\Pi/d\Phi)$, will be discontinuous at the double-layer edge. We thus have

$$\Pi \approx -\alpha\Phi \,,$$

$$(\Phi \gtrsim 0)$$

$$\frac{d^2\Phi}{dZ^2} = -\frac{d\Pi}{d\Phi} \approx \alpha \,, \tag{51}$$

which can be solved to yield

$$\Phi \approx \frac{1}{2} \alpha Z^2 \quad (\Phi \geq 0) \,. \tag{52}$$

From Eq. (52), we see that a finite distance is required for the potential to vary from zero to a given non-zero value.

If the reflected particles are warm there will be no discontinuity in ρ at the double-layer edge. We thus have

$$\Pi \approx -\beta\Phi^2 \,,$$

$$(\Phi \gtrsim 0) \tag{53}$$

$$\frac{d^2\Phi}{dZ^2} = -\frac{d\Pi}{d\Phi} \approx 2\beta\Phi \,,$$

which yields

$$\Phi = \gamma \, \exp\left((2\beta)^{1/2}Z\right) \quad (\Phi \geq 0) \,. \tag{54}$$

The exponential dependence in Eq. (54) indicates that the potential approaches zero for any finite Z , but attains it only asymptotically at $Z = -\infty$.

The behavior at $\Phi = 0$ is determined by the reflected ions in Plasma 1; similar arguments apply at $\Phi = \Phi_0$, with the behavior dependent on the reflected electrons in Plasma 2. Therefore, with warm reflected particles, the double-layer is infinitely long, i.e., electrical

18

neutrality obtains only at $Z = \pm \infty$, even though most of the potential variation occurs over a finite length. A general method of defining the length of a double-layer is thus required.

Andrews & Allen (1971) define the double-layer length as the distance over which the potential varies from a tenth of the trapped ion temperature on the low potential side to within a tenth of the trapped electron temperature on the high potential side of its asymptotic value. Hasan & ter Haar (1978) measure between points on both sides of the double-layer where the potential is within a tenth of the trapped electron temperature of its asymptotic value. Knorr & Goertz (1974) assume a hyperbolic tangent form for their analysis of a double-layer, $\Phi = \Phi_0 \tanh(x/\xi)$, and therefore have the built-in length scale, ξ .

We choose to define the characteristic length, L , of a double-layer as the length over which the constant electric field evaluated at $\Phi_0/2$ would have to exist in order to produce the potential difference Φ_0 , as indicated by the dashed lines in figure 3 ,

$$L \equiv \frac{\Phi_0}{\left| E\left(\frac{\Phi_0}{2}\right) \right|} = \frac{\Phi_0}{\left(-2\Pi\left(\frac{\Phi_0}{2}\right)\right)^{1/2}} . \tag{55}$$

While this definition is no less arbitrary than previous definitions, it commends itself as requiring less numerical integration, and defines the region of strong electric field, over which most of the potential variation occurs.

Applying Eq. (55) to the case of cold particles, the length of the double-layer is found to be

$$L = \frac{\Phi_0}{\left(-2\left[1 - \left(1 + \Phi_0\right)^{1/2} + NQ\left(1 + \frac{2}{Q}\Phi_0\right)^{1/2} - NQ\left(1 + \frac{\Phi_0}{Q}\right)^{1/2}\right]\right)^{1/2}} . \tag{56}$$

When the double-layer is very strong, $\Phi_0 \to \infty \ [N^2Q \to 1$, see Eq. (13)], this reduces to

$$L \simeq 0.92 \ \Phi_0^{3/4} , \tag{57}$$

or, in unnormalized variables,

$$\ell \simeq 0.92 \left(\frac{\epsilon_0^2 e}{m_e}\right)^{1/4} \frac{\phi_0^{3/4}}{\left(en_{el}u_{el}\right)^{1/2}} \quad . \tag{58}$$

This differs by a factor of order unity from Child's Law for a diode, where $en_{el}u_{el}$ is the electron current density. This is consistent with the assumption of a large potential difference, i.e. that the particles enter the double-layer with negligible kinetic energy relative to that with which they leave. We note further that $N^2 Q = 1$ is the normalized form of the Langmuir condition, Eq. (12).

For weak layers, $\phi_0 \to 0 (N \to 1)$, Eq. (56) reduces to

$$L \simeq 2 \left(\frac{Q}{Q+1}\right)^{1/2} \quad , \tag{59}$$

so that the length of very weak double-layers varies smoothly from $L = 0$ to $L = 2$ as Q varies from zero to infinity.

Figure 9 shows the dependence of the length of the double-layer on the parameters describing the adjoining plasmas. In those cases where an increase in one of the temperatures causes a decrease in the potential difference across the double-layer, there is an associated decrease in its length as well.

It is important to note that distances are not normalized to the electron or ion Debye length, but to the distance a transmitted electron travels in a plasma period, before it enters the layer. The scaling is thus independent of temperature. It follows that no difficulty arises in treating the case of cold particles, where the double-layer extends over an infinite number of Debye lengths.

DISCUSSION

It is instructive to apply our model to conditions characteristic of laboratory and space plasmas that may sustain double-layers. Although the physical parameters, i.e. density, temperature, and drift velocity, differ by orders of magnitude, the normalized variables may be similar.

For the double-layers observed by Quon & Wong (1976), we make the rough estimates

$$N \approx 1.2 \ , \ Q \approx 0.5 \ , \ \tau_e \approx 0.2 \ , \ \tau_i \approx 0.1 \ , \ J_e \approx 0.1 \ , \ J_i \approx 0.3 \ , \quad (60)$$

which produce a double-layer of magnitude and length $\Phi_0 = 4.9$, $L = 5.6$. For a density of $10^8 cm^{-3}$, and electron energy of 1 eV in Plasma 1, this corresponds to a potential difference of 20 V with a characteristic distance of 0.3 cm. This is somewhat stronger than the 3-15 V and sharper than the 3-5 cm reported, but of the right order of magnitude.

As we have shown, comparison of the admissibility criteria with the requirement that the reflected particle densities not be negative indicates that reflected particles must be present on both sides of the double-layer. In their experiment, Quon & Wong were able to remove the reflected ion population by biasing a grid appropriately. They report that, without the reflected ions, they could not produce a double-layer.

Although we lack a complete set of measurements made during an active aurora, we assume a current of 1 $\mu A/m^2$ may be carried by a 100 eV electron beam above the double-layer. For parameters

$$N = 1.5 , \quad Q = 0.4, \quad \tau_e = 0.1 \ , \quad \tau = 0.1, \quad J_e = 0.1, \quad J_i = 0.1, \quad (61)$$

(compare with values used by Swift 1976), a double-layer of magnitude and length, $\Phi_0 = 10.3$, $L = 7.4$, results. This corresponds to a 2 kV potential in a 0.7 km long step, which requires an average electric field of 2.8 V/m. This field is a factor of five greater than that measured by satellite (Mozer et al. 1977), but the measurements may not have been made in the center of the double-layer. If the current above the double-layer is carried by 1 keV electrons, the strength of the double-layer increases to 20 kV, while the electric field increases to only 5.0 V/m. These potentials are of the right magnitude to produce the observations of high-energy electron precipitation (see, e.g. Shawhan et al. 1978, and references therein).

For self-consistency the relationships of Eqs. (29) and (47) between the particle energies and temperatures have been developed. If these conditions are not satisfied outside the double-layer, a "pre-sheath" (Schott 1968) may be postulated that would accelerate the particles sufficiently. The excitation of pulses at the ion acoustic speed, as seen in some positive column discharges (Babić & Torvén 1974) may originate in such a pre-sheath.

The reflected particles with non-zero temperature have been assumed to obey Boltzmann's law within the double-layer. This can result either from an isothermal equation of state in a fluid theory approach, or from a Maxwellian velocity distribution in a kinetic theory approach. Non-zero temperature of the transmitted particles has been handled in a fluid theory approach, with an adiabatic equation of state. However, as is shown in Appendix B, the same results can be obtained from a kinetic theory approach with waterbag distribution functions; results for other distribution functions are considered, and compared with the results of fluid theory.

One important aspect of the double-layer that is not treated within this time-independent analysis is that of stability. The Penrose (1960) criterion for determining stability applies only to homogeneous systems. It may thus be possible to find velocity distribution functions that are Penrose stable, but which are unstable due to the inhomogeneity (Wahlberg 1977). Also stability, as determined from the Penrose criterion, depends critically on the distribution functions. As a solution of Poisson's equation, the double-layer is dependent only on the density of the particles, i.e. the integral of the distribution functions. Furthermore, there is evidence from both laboratory (Babić & Torvén 1974; Armstrong 1975; Quon & Wong 1976) and computer experiments (Hubbard & Joyce 1978) that double-layers can co-exist with some instability.

The analysis presented here studies the self-consistency of the double-layer as an independent entity. However, since double-layers form a part of a larger circuit, whether in the laboratory or in space, there are further problems relating to consistency with the external circuit that will require investigation in future work.

APPENDIX A: LIMITS OF FLUID THEORY

For $\gamma \neq 1$ in (36), (37) is rewritten

$$\frac{1}{n} \frac{d}{dx} (nT) = \frac{\gamma}{\gamma-1} \frac{dT}{dx} = \frac{\gamma}{\gamma-1} \frac{d}{dx} \left[\hat{T} \left(\frac{n}{\hat{n}}\right)^{\gamma-1} \right] . \qquad (A.1)$$

The isothermal equation of state, $\gamma = 1$, will be treated separately, below.

The conserved quantity analogous to (40) is

$$\frac{\hat{n}^2 \hat{u}^2}{2n^2} + \frac{q\phi}{m} + \frac{\gamma}{\gamma-1} \frac{\hat{T}}{m} \left(\frac{n}{\hat{n}}\right)^{\gamma-1} = \frac{\hat{u}^2}{2} + \frac{q\hat{\phi}}{m} + \frac{\gamma}{\gamma-1} \frac{\hat{T}}{m} , \qquad (A.2)$$

where q is the charge of the particle, $\hat{u}$ is the drift velocity, $\hat{T}$ is the temperature, and $\hat{\phi}$ is the potential at the reference position. Rearranging (A.2) yields

$$F_\gamma \left(\frac{n}{\hat{n}}\right) = \hat{u}^2 \left(\frac{\hat{n}}{n}\right)^2 + \frac{2\gamma}{\gamma-1} \frac{\hat{T}}{m} \left(\frac{n}{\hat{n}}\right)^{\gamma-1} = \hat{u}^2 + \frac{2q}{m} (\hat{\phi} - \phi) + \frac{2\gamma}{\gamma-1} \frac{\hat{T}}{m} . \qquad (A.3)$$

The function $F_\gamma (n/\hat{n})$ is plotted in figure A.1(a), and shows a minimum at

$$\left(\frac{n}{\hat{n}}\right)_m = \left(\frac{m\hat{u}^2}{\gamma\hat{T}}\right)^{\frac{1}{\gamma+1}} . \qquad (A.4)$$

As $q\phi$ decreases, the density must increase or decrease as indicated in figure A.1 in order to satisfy (A.3). However, decreasing $q\phi$ represents acceleration which, to conserve particle number, must be accompanied by a decrease in the density, n. Values of $n/\hat{n}$ greater than $(n/\hat{n})_m$ are therefore nonphysical. Thus, evaluating (A.4) at the reference position yields

$$\gamma \hat{T} < m\hat{u}^2 . \qquad (A.5)$$

Applying (A.5) to the electrons entering the double-layer from their reference point in Plasma 1, or to the ions entering from their reference point in Plasma 2, and normalizing as in (41), yields

$$\gamma \tau_e < 1 \ , \quad \gamma \tau_i < 0 \ , \tag{A.6}$$

which, for $\gamma = 3$, gives (43).

For $\gamma = 1$, (A.1) takes the form

$$\frac{1}{n} \frac{d}{dx} (nT) = \hat{T} \frac{d}{dx} (\ln n) \ , \tag{A.7}$$

so that (A.2) becomes

$$\frac{\hat{n}^2 \hat{u}^2}{2n^2} + \frac{q\phi}{m} + \frac{\hat{T}}{m} \ln n = \frac{\hat{u}^2}{2} + \frac{q\hat{\phi}}{m} + \frac{\hat{T}}{m} \ln \hat{n} \ . \tag{A.8}$$

Collecting terms in $n/\hat{n}$ yields

$$F_1 \left(\frac{n}{\hat{n}} \right)^2 = \hat{u}^2 \left(\frac{\hat{n}}{n} \right)^2 + 2 \frac{\hat{T}}{m} \ln \left(\frac{n}{\hat{n}} \right) = \hat{u}^2 + \frac{2q}{m} (\hat{\phi} - \phi) \ , \tag{A.9}$$

which is plotted in figure A.1(b), and has its minimum at

$$\left(\frac{n}{\hat{n}} \right)_m = \left(\frac{m\hat{u}^2}{\hat{T}} \right)^{1/2} \ . \tag{A.10}$$

This is the result of (A.4) for $\gamma = 1$, and therefore implies the temperature limitations of (A.6) again.

APPENDIX B: COMPARISON OF FLUID AND KINETIC MODELS
FOR TRANSMITTED PARTICLES

Instead of using a fluid model for the transmitted particles, and then assuming an equation of state, it is possible to assume a form for the velocity distribution function, $f(u)$, before the particles enter the double-layer, and determine its dependence on the potential, ϕ, by the Vlasov equation. Taking $f(u)$ as time-independent, the Vlasov equation, in one dimension, is satisfied for any distribution that is a function of the total energy;

$$f(u,\phi) = f\left\{ \pm \left[u^2 + \frac{2q\phi}{m} \right]^{1/2} \right\} , \tag{B.1}$$

where m and q are the mass and charge of the particle. The spatial dependence of f enters through the potential, ϕ. The sign of the argument in (B.1) is the sign of the velocity.

A simple choice for the distribution function at $\phi=0$ is a waterbag with all particles forward-going, [see figure B.1(a)]

$$f(u,0) = \begin{cases} \dfrac{3^{1/2}}{6} \dfrac{n_0}{u_t} & |u-u_D| < 3^{1/2} u_t , \\ \\ 0 & |u-u_D| > 3^{1/2} u_t . \end{cases} \tag{B.2}$$

The identifications of n_0 as the density, u_D as the drift velocity, and u_t as the thermal velocity, are made by calculating the appropriate moments of the distribution.

Normalizing the density and potential, and defining a temperature consistent with §4,

$$N = \frac{n}{n_0} \quad , \quad \phi = -\frac{q\phi}{mu_D^2} \quad , \quad \tau = \frac{u_t^2}{u_D^2} \quad , \tag{B.3}$$

the density as a function of ϕ is

$$N(\phi) = \frac{3^{1/2}}{6\tau^{1/2}} \left\{ \left[\left(1 + (3\tau)^{1/2} \right)^2 + 2\phi \right]^{1/2} - \left[\left(1 - (3\tau)^{1/2} \right)^2 + 2\phi \right]^{1/2} \right\} . \tag{B.4}$$

25

which is equivalent to (42) for electrons. The assumption of all forward-going particles is

$$3\tau < 1 ,\qquad\qquad (B.5)$$

which is (43) for the use of fluid theory. Thus as far as the analysis in §4 is concerned, the waterbag and fluid models are identical.

If the velocity distribution is allowed to have some backward-going particles, as in figure B.1(b), the density, normalized according to (B.3) is

$$N(\Phi) = \frac{3^{1/2}}{6\tau^{1/2}}\left\{\left[\left(1 + (3\tau)^{1/2}\right)^2 + 2\Phi\right]^{1/2} + \left[\left(1 - (3\tau)^{1/2}\right)^2 + 2\Phi\right]^{1/2} - (8\Phi)^{1/2}\right\} .$$

$$(B.6)$$

Although the mathematics does not allow the general case of a drifting Maxwellian to be treated analytically, two particular cases can be studied. If the distribution is as in figure B.1(c), a Maxwellian with a large drift-to-thermal velocity ratio, and thus with a negligible number of backward-going particles, the distribution function is

$$f(u,0) = \frac{n_0}{u_t(2\pi)^{1/2}} \exp\left[-\frac{(u-u_D)^2}{2u_t^2}\right] ,\qquad\qquad (B.7)$$

To second order in τ, the normalized density is

$$N(\Phi) = \frac{1}{(1 + 2\Phi)^{1/2}}\left[1 - \frac{3\Phi\tau}{(1 + 2\Phi)^2} + \frac{15}{2}\frac{(3\Phi-2)\Phi\tau^2}{(1 + 2\Phi)^4}\right] .\qquad (B.8)$$

This agrees to first order with the small-τ expansion of N for the fluid/waterbag model, the second order term of (B.8) being larger by a factor of 5/3 than in the fluid/waterbag model.

For the forward-going half of a Maxwellian at $\phi=0$, illustrated in figure B.1(d), the distribution function, drift velocity and thermal velocity are

$$f(u,0) = \begin{cases} \dfrac{n_0}{u_0} \left(\dfrac{2}{\pi}\right)^{1/2} \exp\left(-\dfrac{u^2}{2u_0^2}\right) & (u > 0) , \\[2em] 0 & (u < 0) , \end{cases}$$

$$u_D = u_0 \left(\frac{2}{\pi}\right)^{1/2} \simeq 0.80\, u_0 ,$$

$$u_t = u_0 \left(\frac{\pi-2}{\pi}\right)^{1/2} \simeq 0.60\, u_0 . \tag{B.9}$$

It can be seen from (B.9) that the normalized temperature is a constant, $\tau = (\pi-2)/2 \simeq 0.57$. The normalized density, as the particles are accelerated, is

$$N(\Phi) = \exp\left(\frac{\Phi}{\tau}\right)\left[1 - \mathrm{erf}\left(\left(\frac{\Phi}{\tau}\right)^{1/2}\right)\right] . \tag{B.10}$$

Figure B.2 shows the dependence of the density on the potential for the various distribution functions considered here. For all but $\tau = 0.3$, the fluid/waterbag and Maxwellian curves totally overlap; the Maxwellian is the lower of the $\tau = 0.3$ curves. Since Poisson's equation depends only on the density, and not on the detailed shape of the distribution, the fluid/waterbag model may be used for a Maxwellian with a large drift-to-thermal velocity ratio, but not for a half-Maxwellian.

REFERENCES

ALFVÉN, H. & CARLQVIST, P. 1967 Solar Phys., 1, 220.

ANDERSSON, D., BABIĆ, M., SANDAHL, S. & TORVÉN, S. 1969 Proceedings 9th International Conference on Phenomena in Ionized Gases, p. 142, Acad. Soc. Rep. Rumania.

ANDREWS, J. G. & ALLEN, J. E. 1971 Proc. Roy. Soc. Lond. A., 320, 459.

ARMSTRONG, R. J. 1975 Proceedings 12th International Conference on Phenomena in Ionized Gases, p. 124, North-Holland.

ARMSTRONG, R. J. & TORVÉN, S. 1974 Report No. 10-74, The Auroral Observatory, Tromsø.

BABIĆ, M. & TORVÉN, S. 1974 TRITA-EPP-74-02, Royal Institute of Technology, Dept. of Electron Physics, Stockholm.

BLOCK, L. P. 1972 Cosmic Electrodynamics, 3, 349.

BOHM, D. 1949 The Characteristics of Electrical Discharges in Magnetic Fields (eds. A. Guthrie & R. K. Wakerling), p. 77, McGraw-Hill.

CARLQVIST, P. 1969 Solar Phys., 7, 377.

CARLQVIST, P. 1978 Astrophys. Space Sci. Library, Reidel (in press).

COAKLEY, P., HERSHKOWITZ, N., HUBBARD, R. & JOYCE, G. 1978 Phys. Rev. Lett., 40, 230.

CRAWFORD, F. W. & CANNARA, A. B. 1965 J. Appl. Phys., 36, 3135.

CRAWFORD, F. W. & FREESTON, I. L. 1963 Proceedings 6th International Conference on Phenomena in Ionized Gases, p. 461, SERMA.

DeGROOT, J. S., BARNES, C., WALSTEAD, A. E. & BUNEMAN, O. 1977 Phys. Rev. Lett., 38, 1283.

GOERTZ, C. K. & JOYCE, G. 1975 Astrophys. Space Sci., 32, 165.

HASAN, S. S. & ter HAAR, D. 1978 Astrophys. Space Sci., 56, 89.

HUBBARD, R. F. & JOYCE, G. 1978 Report 78-37, Univ. of Iowa, Dept. of Physics and Astronomy, Iowa City.

JACOBSEN, R. A. & EUBANK, H. P. 1973 Plasma Phys., 15, 243.

JOYCE, G. & HUBBARD, R. F. 1978 J. Plasma Phys., 20, 391.

KAN, J. R. 1975 J. Geophys. Res., 80, 2089.

KNORR, G. & GOERTZ, C. K. 1974 Astrophys. Space. Sci., 31, 209.

LANGMUIR, I. 1929 Phys. Rev., 33, 954.

LEVINE, J. S., ILIĆ, D. B. & CRAWFORD, F. W. 1978 J. Geomag. Geoelectr. 30, 461.

LUTSENKO, E. I., SEREDA, N. D. & KONTSEVOI, L. M. 1975 Zh. Tekh. Fiz., 45, 789; 1976 Sov. Phys. Tech. Phys., 20, 498.

MONTGOMERY, D. & JOYCE, G. 1969 J. Plasma Phys., 3, 1.

MOZER, F. S., CARLSON, C. W., HUDSON, M. K., TORBERT, R. B., PARADY, B., YATTEAU, J. & KELLEY, M. C. 1977 Phys. Rev. Lett., 38, 292.

PENROSE, O. 1960 Phys. Fluids, 3, 258.

PREWETT, P. D., & ALLEN, J. E. 1976 Proc. Roy. Soc. Lond. A, 348, 435.

QUON, B. H. & WONG, A. Y. 1976 Phys. Rev. Lett., 37, 1393.

SANDAHL, S. 1971 Physica Scripta, 3, 275.

SCHOTT, L. 1968 Plasma Diagnostics (ed. W. Lochte-Holtgreven), p. 684, North-Holland.

SHAWHAN, S. D., FÄLTHAMMAR, C.-G. & BLOCK, L. P. 1978 J. Geophys. Res., 83, 1049.

SMITH, R. A. & GOERTZ, C. K. 1978 J. Geophys. Res., 83, 2617.

SWIFT, D. W. 1975 J. Geophys. Res., 80, 2096.

SWIFT, D. W. 1976 J. Geophys. Res., 81, 3935.

TORVÉN, S. 1978 Astrophys. Space Sci. Library, Reidel (in press).

TORVÉN, S. & ANDERSSON, D. 1978 TRITA-EPP-78-12, Royal Institute of Technology, Depts. of Plasma and Electron Physics, Stockholm.

WAHLBERG, C. 1977 J. Plasma Physics, 18, 415.
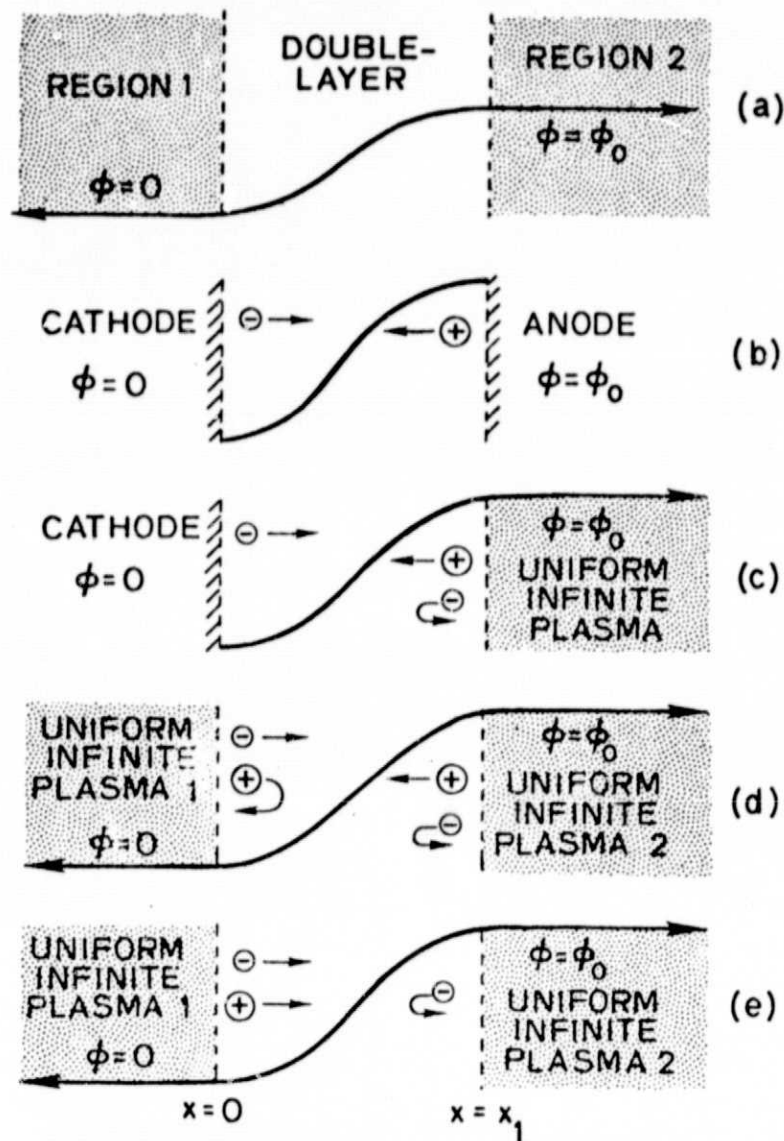
FIG. 1. Various double-layer models.

(a) Transition region between two plasmas with a potential difference.

(b) Space-charge-limited diode. (Particles enter with zero velocity, but with non-zero flux.)

(c) Space-charge-limited cathode (Cathodic electrons enter with zero velocity, but with non-zero flux. Plasma electrons are reflected by the double-layer; ions are transmitted through it.)

(d) Double-layer between two plasmas. (Four species of particles are reflected and transmitted.)

(e) Double-layer between two plasmas. (Ions from Plasma 1 are transmitted by the double-layer. Only one species of particles is reflected: electrons in Plasma 2.)
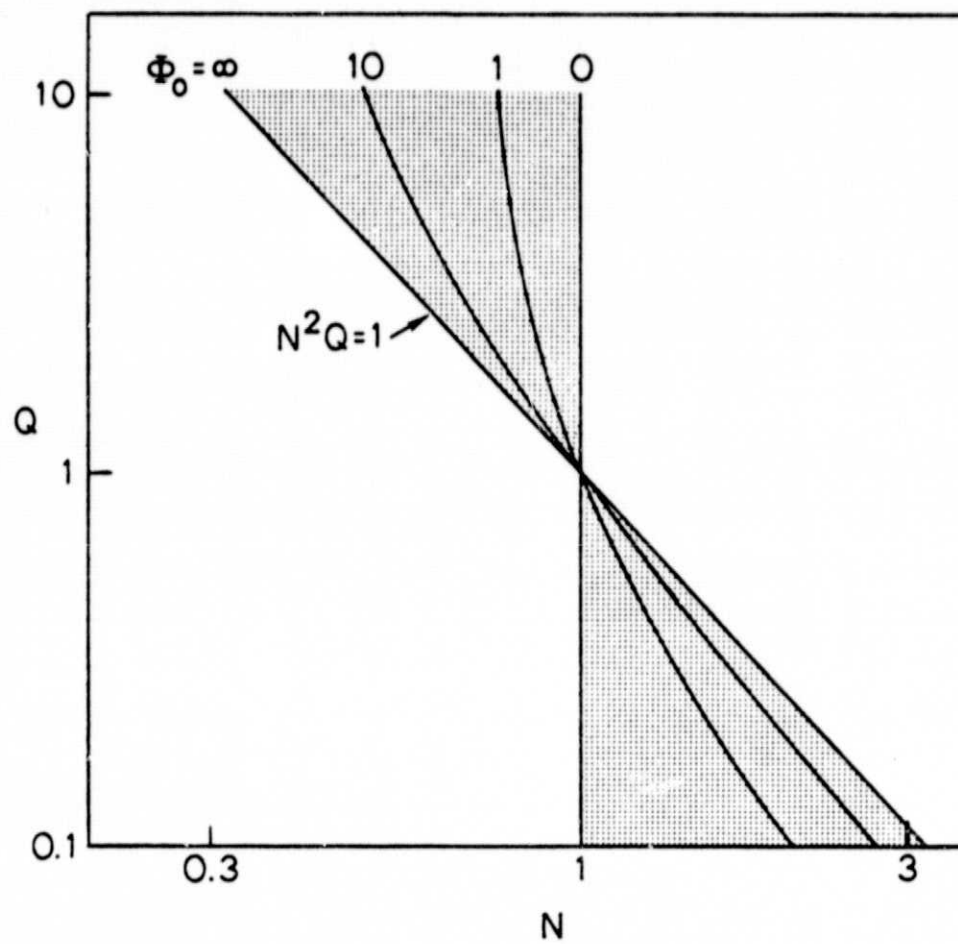
FIG. 2. Double-layer regions: Cold plasma theory.
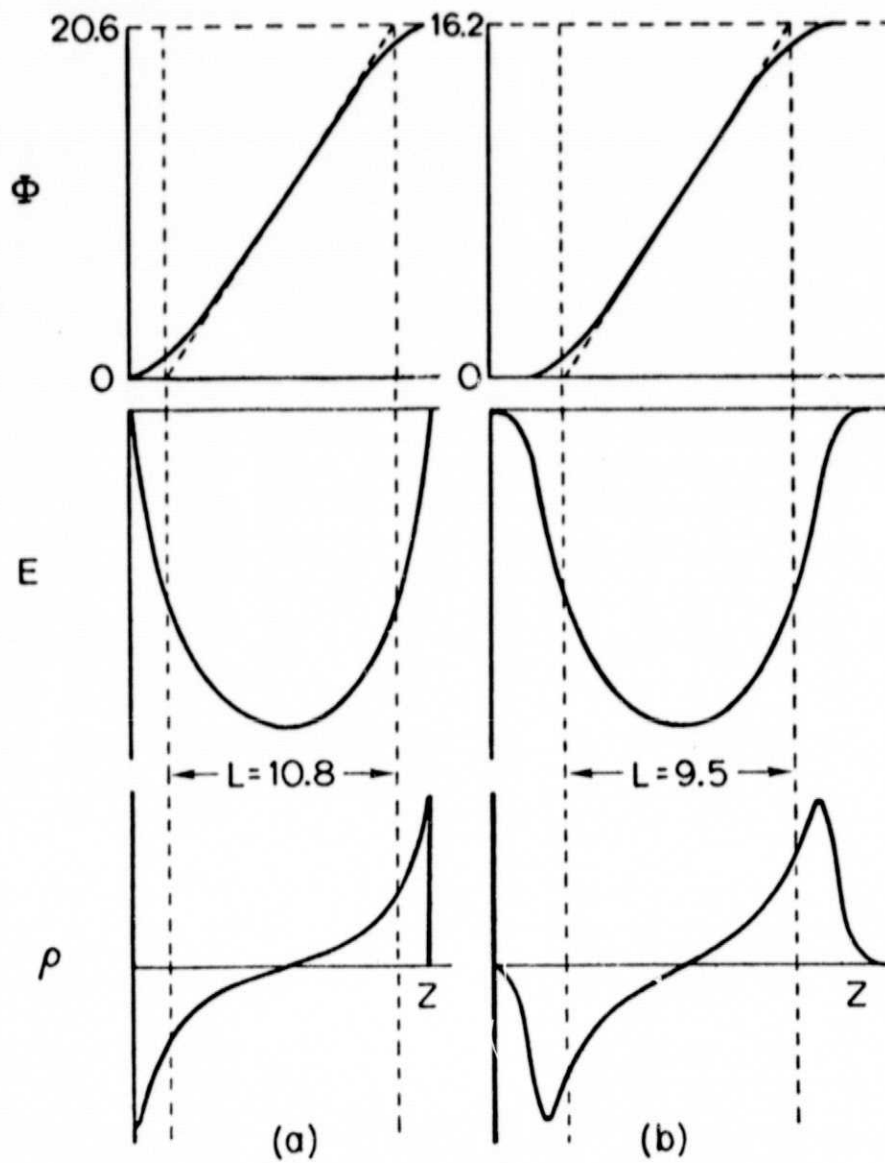
FIG. 3. Double-layer characteristics (N = 1.1, Q = 0.8).
(a) Cold Plasma theory ($J_e = J_i = 0$).
(b) Macroscopic plasma theory ($J_e = J_i = 0.1$).
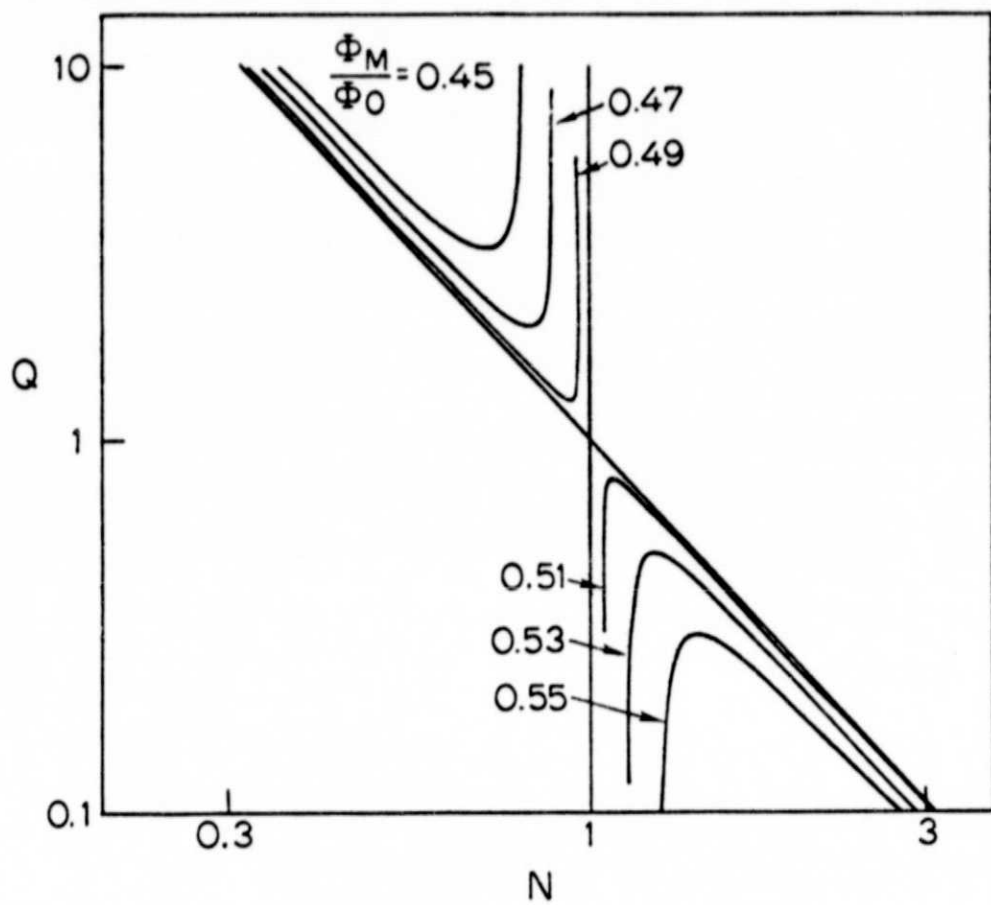
FIG. 4. Normalized potential (Φ_M/Φ_0) at location of maximum electric field in a double-layer: cold plasma theory.
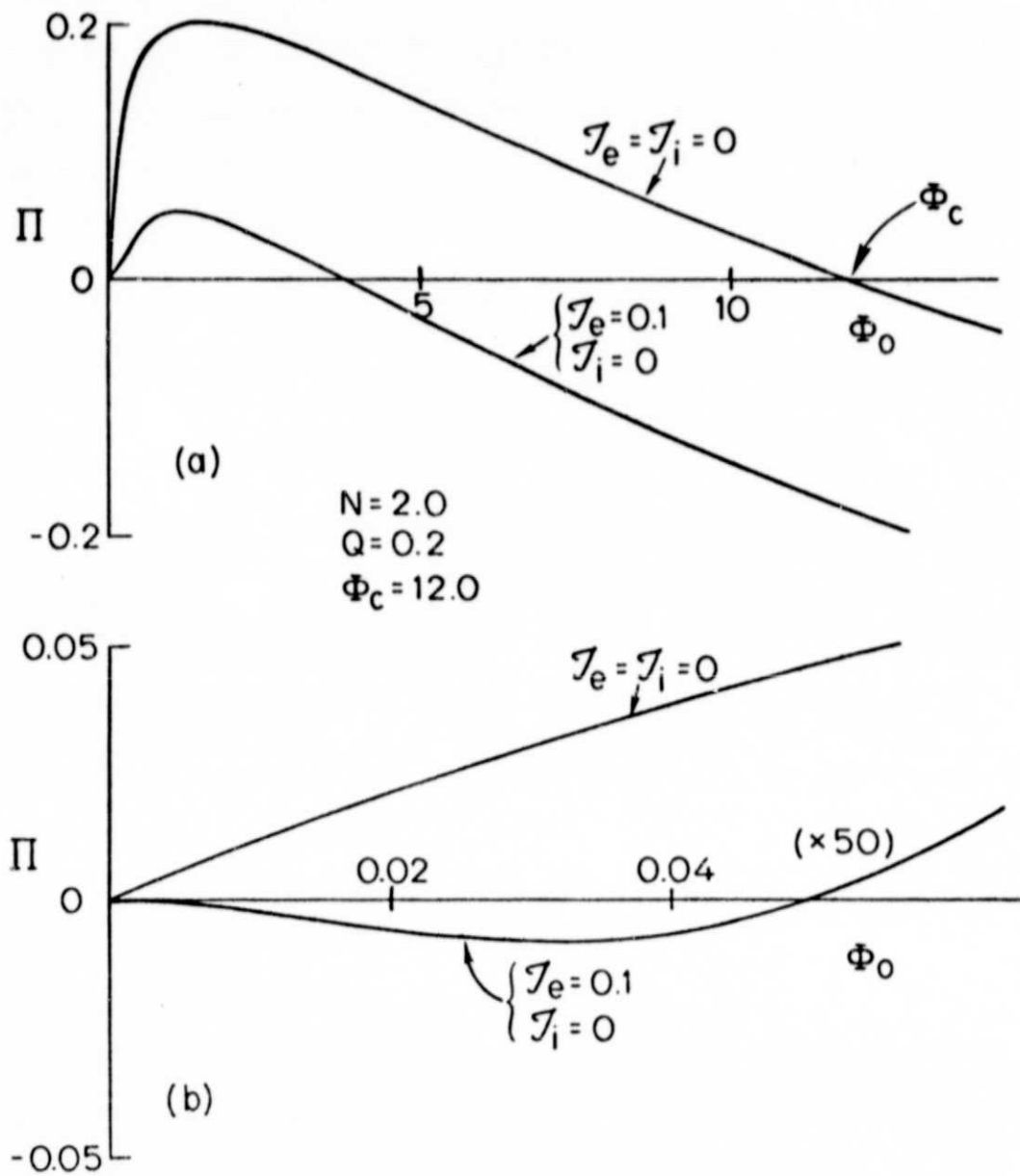
FIG. 5. Double-layer solutions for non-zero reflected particle
          temperatures.

(a) Modification of cold plasma solution.

(b) Additional solution.
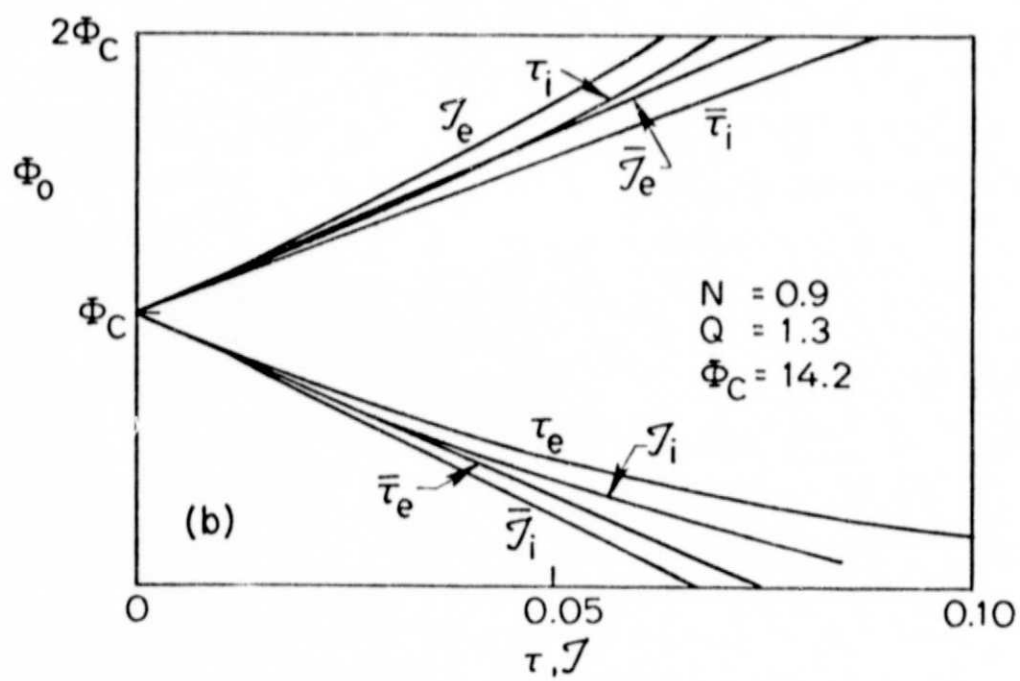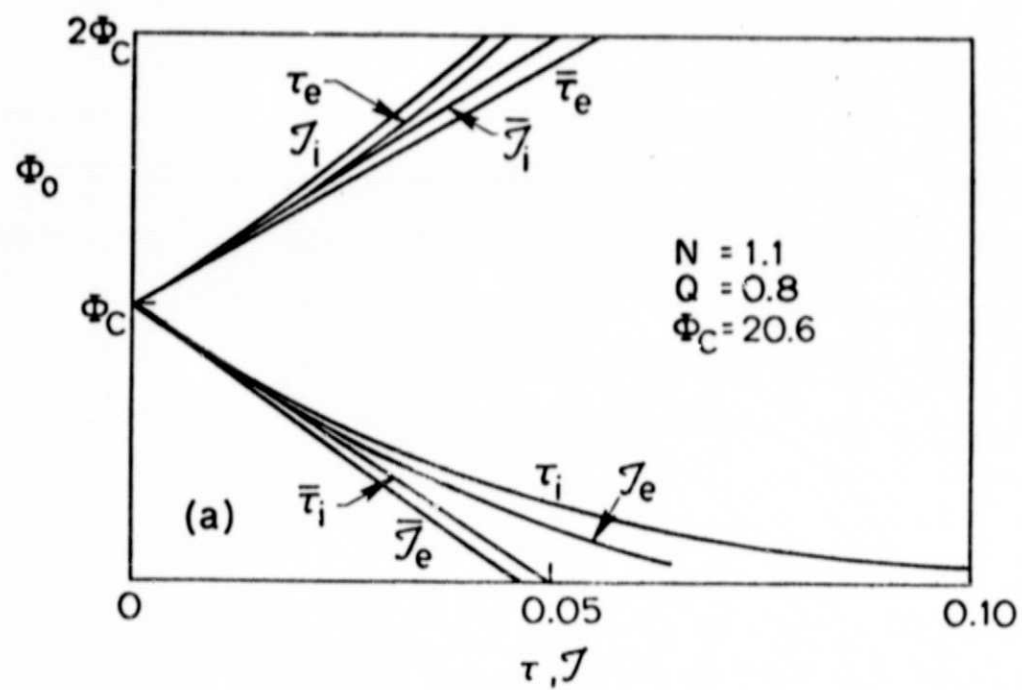
FIG. 6. Variation of double-layer potential (Φ_0)
with separate variation of particle temperatures.
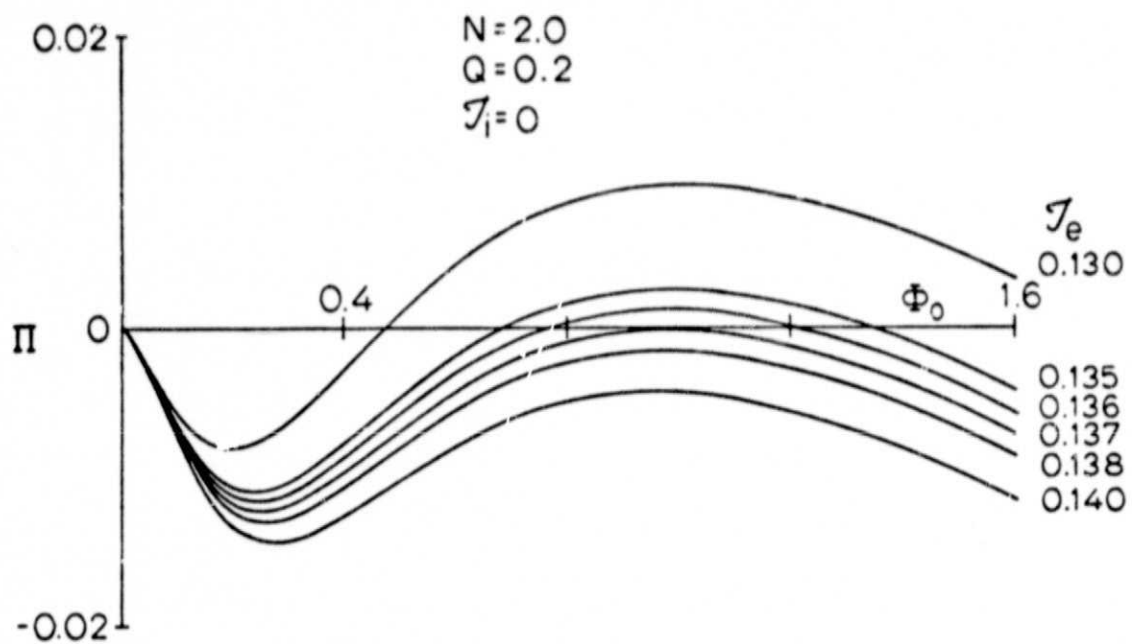
FIG. 7. Effect of reflected particle temperature variation on double-layer solutions $\left(\Pi(\Phi_0) = 0 \right)$.
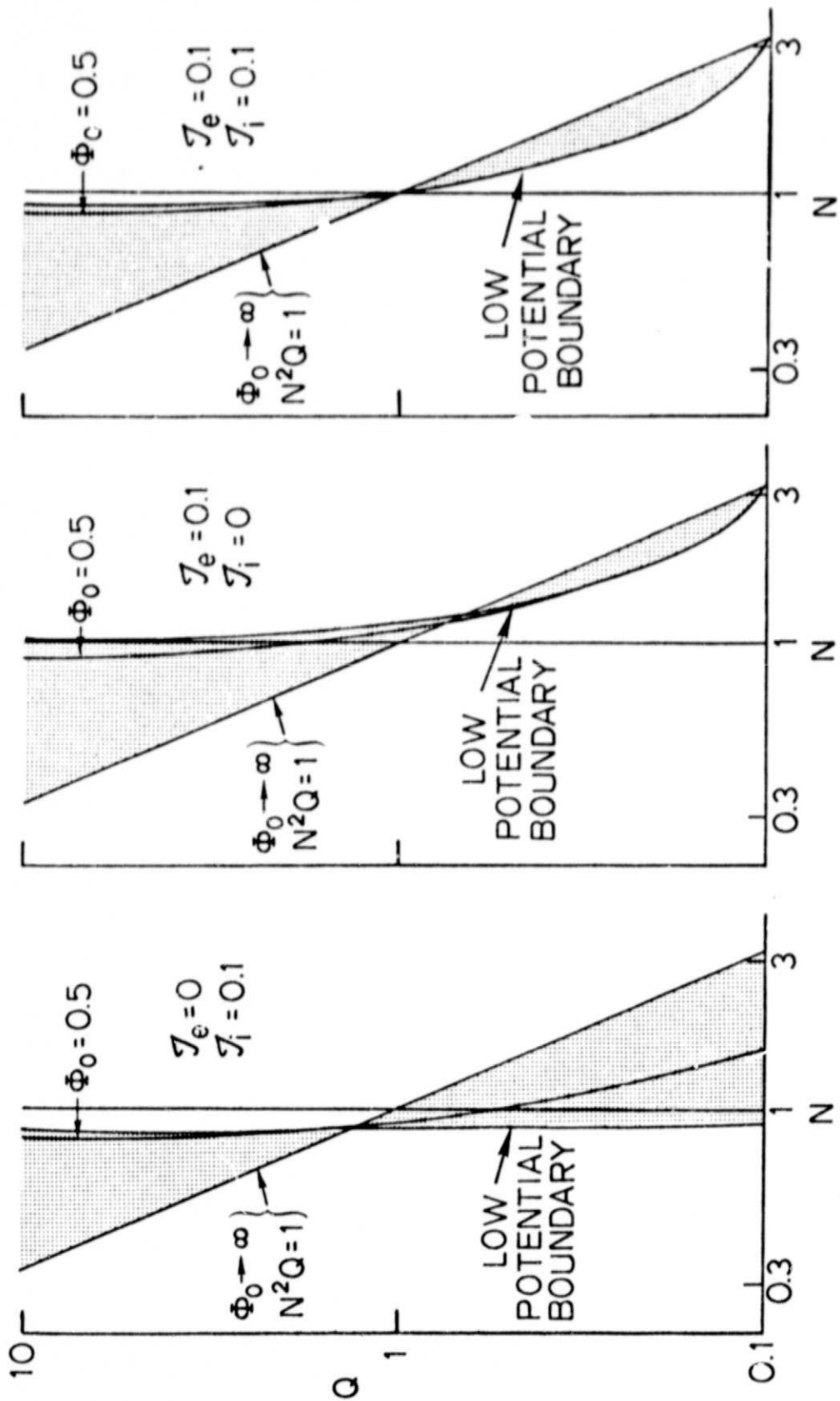
FIG. 8. Double-layer region: non-zero reflected particle temperatures.
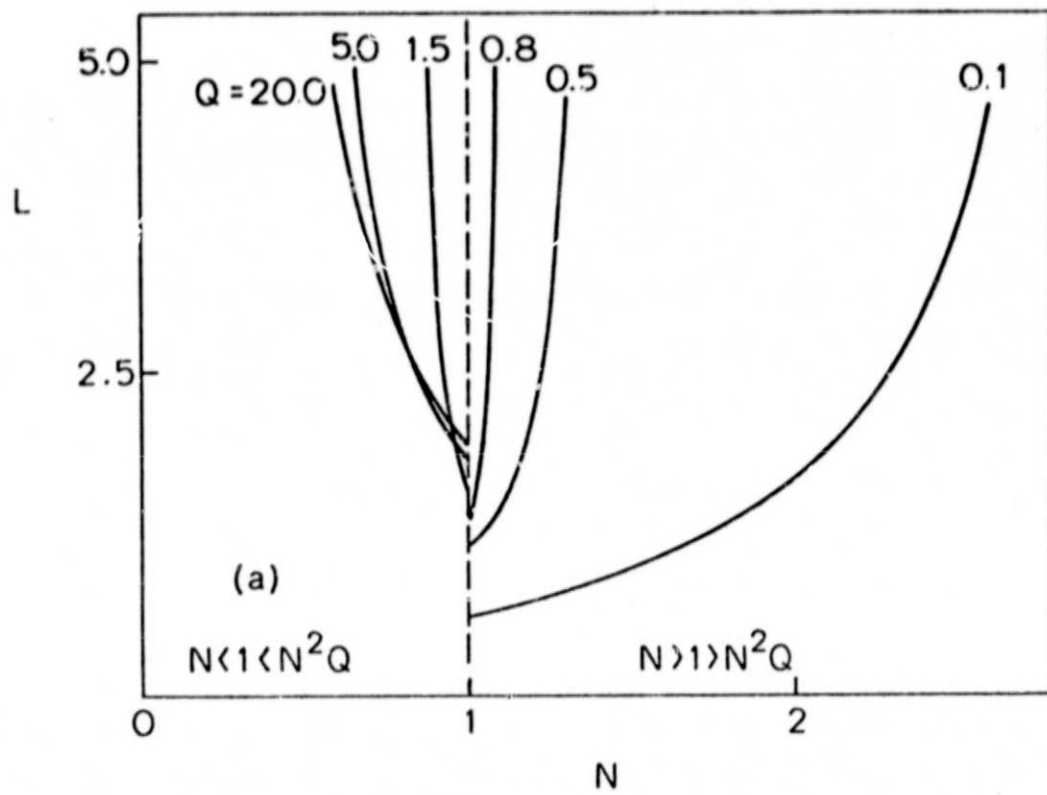
FIG. 9.   Double-layer length.
         (a)   Cold plasma theory.
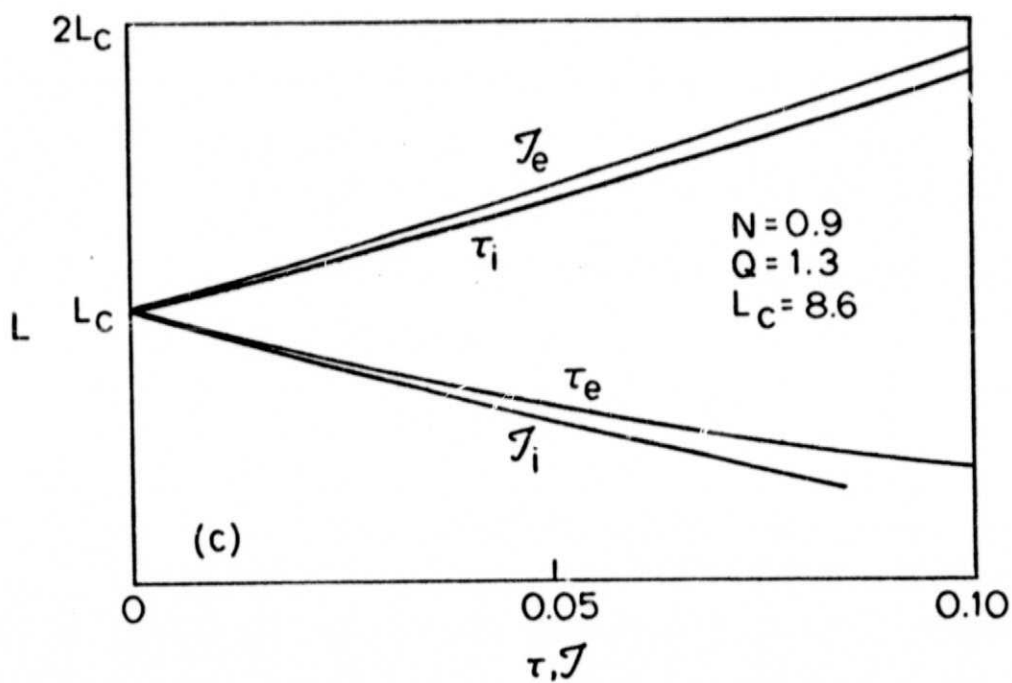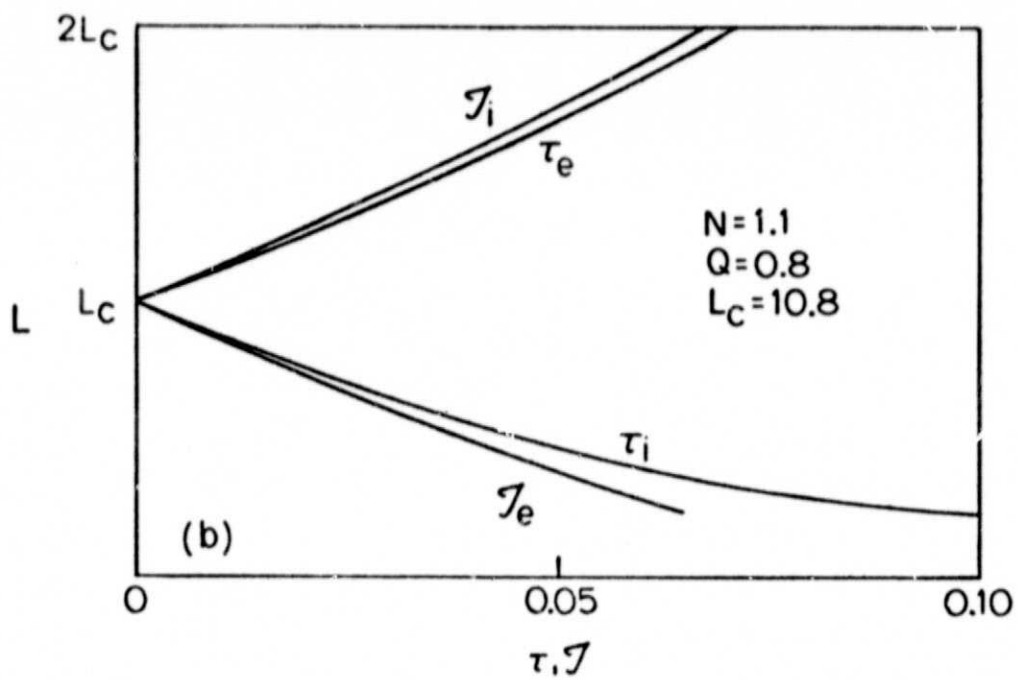
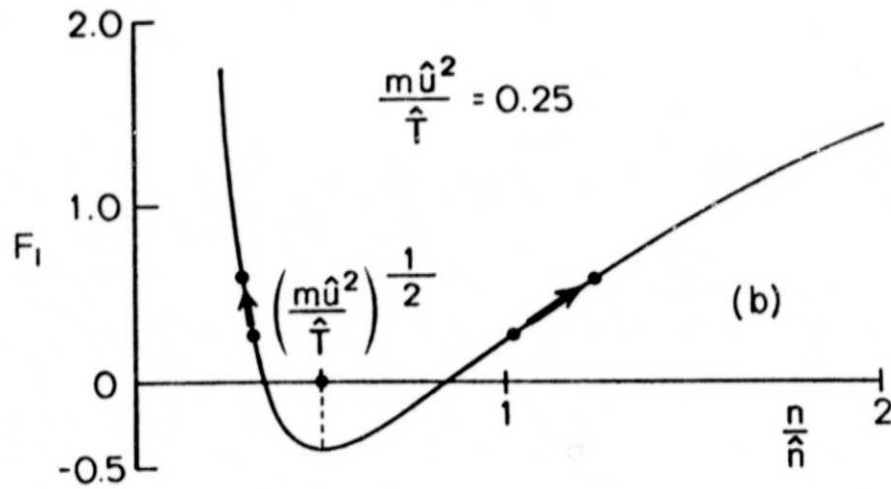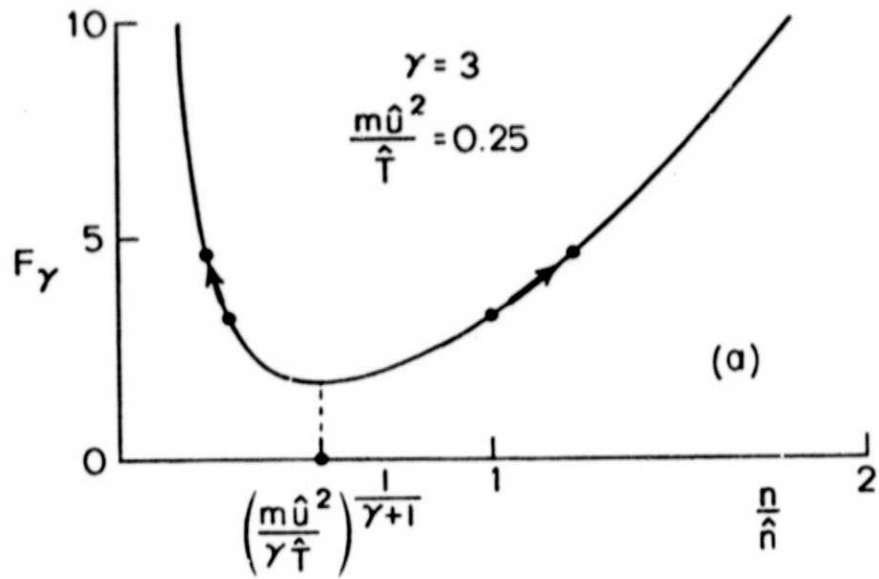FIG. 9. (Contd.) Double-layer length.

(b), (c) Macroscopic plasma theory.

FIG. A.1. Variation of functions F_γ and F_1
(Arrows correspond to $q\phi$ decreasing).
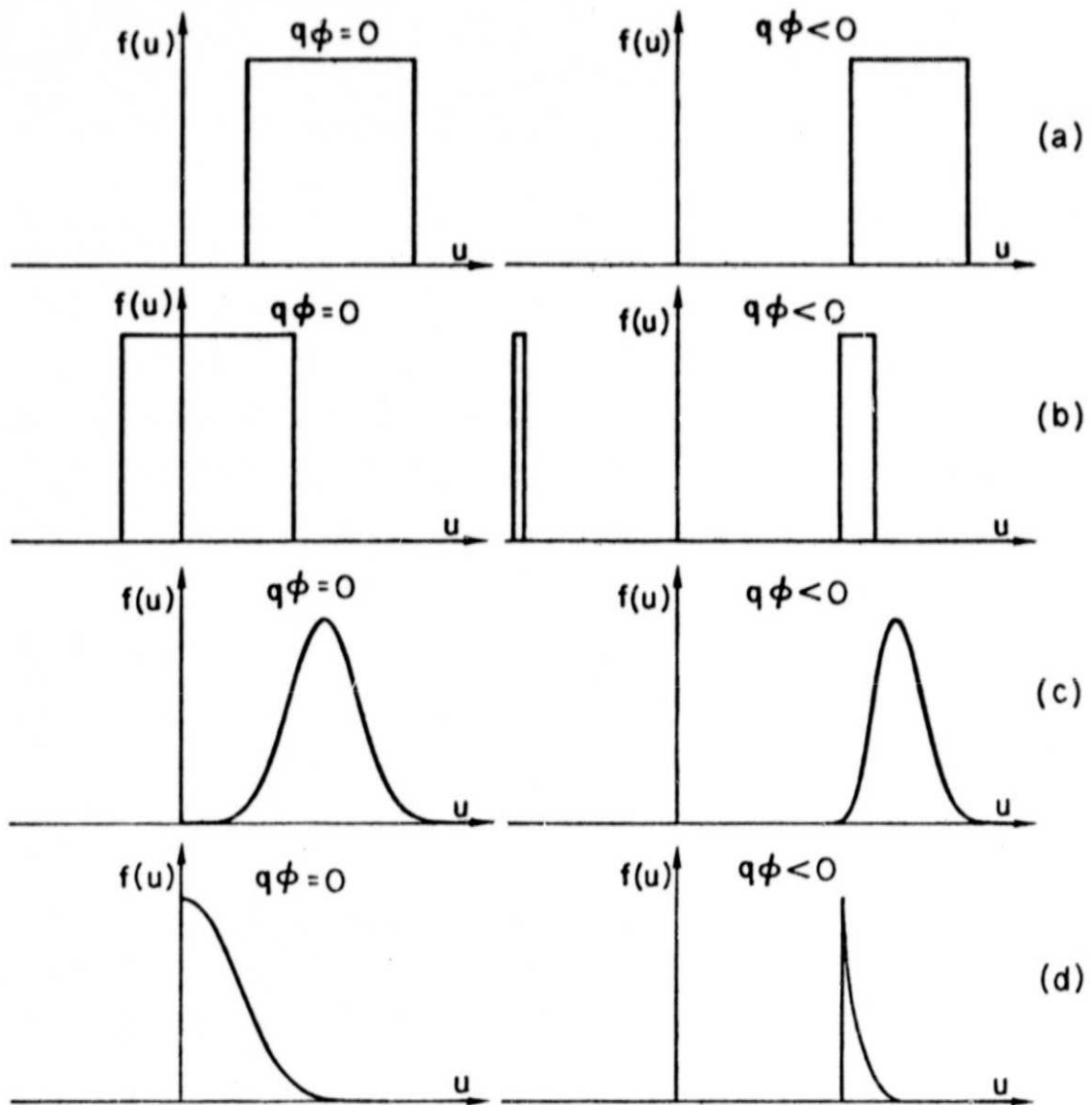
(a) Adiabatic.

(b) Isothermal.

FIG. B.1. Velocity distribution functions at $q\phi = 0$ and $q\phi < 0$.

    (a)   Waterbag with all particles forward-going.

    (b)   Waterbag with forward- and backward-going particles.

    (c)   Maxwellian with large drift-to-thermal velocity ratio.
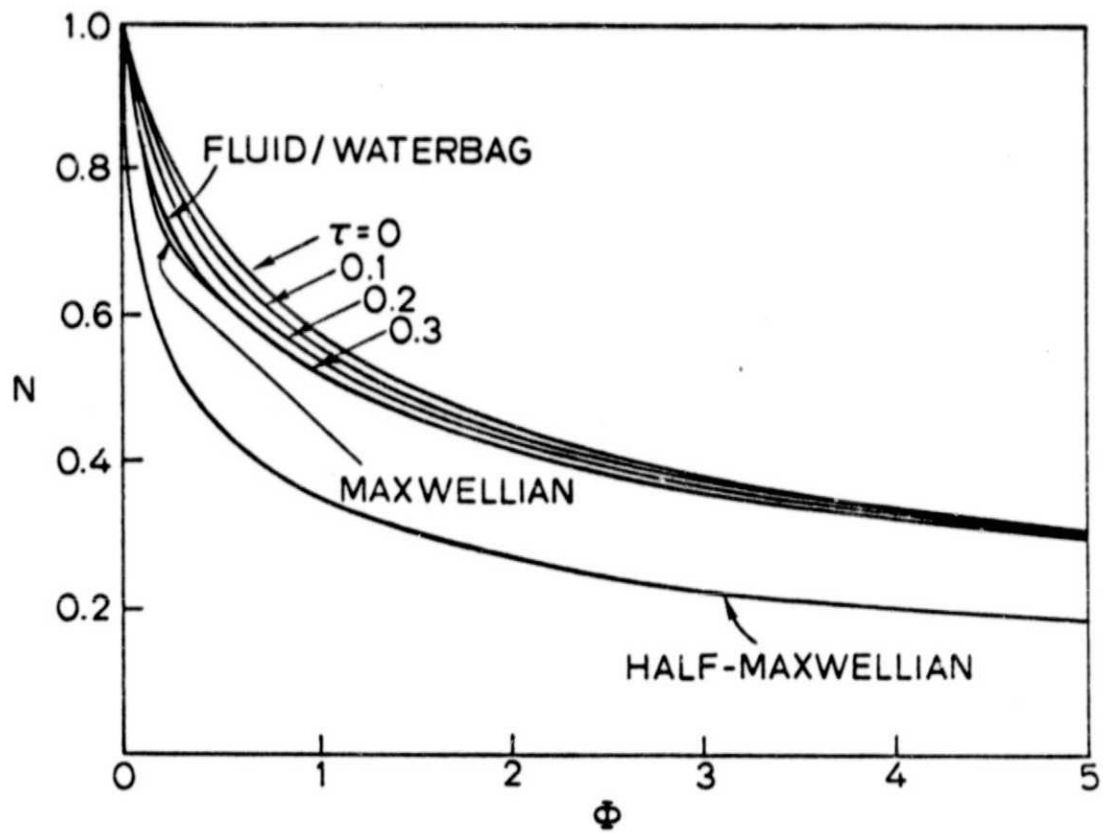
    (d)   Half-Maxwellian.

FIG. B.2. Variation of $N(\Phi)$ for the velocity distribution functions of figure B.1.